

OSCILLATORY ZONED LIDDICOATITE FROM ANJANABONOINA, CENTRAL MADAGASCAR. I. CRYSTAL CHEMISTRY AND STRUCTURE BY SREF AND ^{11}B AND ^{27}Al MAS NMR SPECTROSCOPY

AARON J. LUSSIER, YASSIR ABDU AND FRANK C. HAWTHORNE[§]

Department of Geological Sciences, University of Manitoba, Winnipeg, Manitoba R3T 2N2, Canada

VLADIMIR K. MICHAELIS, PEDRO M. AGUIAR AND SCOTT KROEKER

Department of Chemistry, University of Manitoba, Winnipeg, Manitoba R3T 2N2, Canada

ABSTRACT

The crystal structures of 23 samples extracted from a large slice oriented along (001) of a single crystal of liddicoatite from the Anjanabonoina granitic pegmatite in Madagascar (showing pronounced, visually discontinuous oscillatory zones and anomalous biaxiality) were refined to $R1$ indices of 1.5–2.9% ($\langle R_1 \rangle = 1.78\%$). Cell parameters are in the range $a \approx 15.82\text{--}15.87$, $c \approx 7.10\text{--}7.12$ Å. Spindle-stage measurement of $2V$ gave values of 0.0° for a fragment from the (001) zone and $8(3)$ and $18.9(5)^\circ$ for fragments from the pyramidal zone of the crystal. However, single-crystal X-ray intensity data show no deviation from $3m$ Laue symmetry, indicating that there is no information in the diffraction data on any deviation from $R3m$ symmetry. The $\langle T\text{-O} \rangle$ distances are in the range $1.616\text{--}1.619$ Å, with a grand mean value of $1.6175(7)$ Å. The occupancy of the T site was expressed as $x\text{Si} + (1-x)\text{B}$, and x was treated as variable in the refinement procedure. The effect of using different scattering factors (*i.e.*, ionized *versus* neutral) on the refined site-occupancies was investigated in detail. The grand mean refined $^{[4]}\text{B}$ content of the T site varies from -0.04 apfu for ionized scattering-curves for O and Si to 0.25 apfu for neutral scattering-curves for O and Si, illustrating the effect of the use of different scattering curves on refined $^{[4]}\text{B}$ site-populations. Examination of $\langle T\text{-O} \rangle$ distances as a function of aggregate cation radius for tourmalines containing $^{[4]}\text{B}$ and $^{[4]}\text{Al}$ shows a large amount of scatter, emphasizing the need for more accurate data. The limits of detection for ^{11}B and ^{27}Al in tourmaline by Magic-Angle-Spinning Nuclear Magnetic Resonance (MAS NMR) spectroscopy were investigated by simulation. For minimum (<0.04 apfu) and maximum (0.12 apfu) contents of (paramagnetic) transition metals, the limits of detection of $^{[4]}\text{B}$ are ~ 0.02 and 0.08 apfu , and of $^{[4]}\text{Al}$ are ~ 0.01 and 0.01 apfu , respectively. ^{11}B and ^{27}Al MAS NMR spectroscopy gave no evidence of the presence of tetrahedrally coordinated B or Al at the T site above these detection limits in any sample. This result is in accord with our refinement results using an ionized scattering-curve for O and a neutral scattering-curve for Si, suggesting that use of these curves is giving more accurate results than refinement with neutral scattering factors. The $\langle Z\text{-O} \rangle$ distances are in the range $1.904\text{--}1.907$ Å, with a grand mean value of $1.9047(8)$ Å, and structure refinement indicates site-scattering values in accord with complete occupancy of the Z site by Al. Hence throughout this complexly zoned crystal, $\text{Si} = 6.00$ apfu and $^Z\text{Al} = 6.00$ apfu .

Keywords: liddicoatite, elbaite, tourmaline, oscillatory zoning, crystal-structure refinement, electron-microprobe analysis, magic-angle-spinning nuclear magnetic resonance spectroscopy, Mössbauer spectroscopy, site populations, Anjanabonoina, Madagascar.

SOMMAIRE

Nous décrivons la structure cristalline de 23 fragments extraits d'une section orientée le long de (001) d'un monocrystal de liddicoatite provenant de la pegmatite granitique d'Anjanabonoina, au Madagascar, et affinés jusqu'à un résidu $R1$ dans l'intervalle 1.5–2.9% ($\langle R_1 \rangle = 1.78\%$). Ce cristal montre des zones oscillatoires discontinues et une biaxialité anomale. Les paramètres réticulaires ont des valeurs dans les intervalles suivants: $a \approx 15.82\text{--}15.87$, $c \approx 7.10\text{--}7.12$ Å. Les mesures de $2V$ utilisant ces fragments sur tige orientable ont donné des valeurs de 0.0° pour un fragment provenant de la zone (001), et $8(3)$ et $18.9(5)^\circ$ pour des fragments pris de la zone pyramidale. Toutefois, les données portant sur les intensités en diffraction X ne révèlent aucune déviation de la symétrie de Laue $3m$, ce qui montre qu'il n'y a aucune information concernant un écart de la symétrie $R3m$ dans ces données. Les distances $\langle T\text{-O} \rangle$ tombent dans l'intervalle $1.616\text{--}1.619$ Å, avec une moyenne globale de $1.6175(7)$ Å. L'occupation du site T est exprimée sous forme $x\text{Si} + (1-x)\text{B}$, et nous avons traité x comme une variable au cours des affinements. Le fait d'utiliser des facteurs de dispersion différents, c'est-à-dire des facteurs prévus pour des atomes neutres

[§] E-mail address: frank_hawthorne@umanitoba.ca

ou des ions, exerce une influence sur les occupations affinées des sites. La teneur moyenne globale en $[^{14}\text{B}]$ des sites T varie de ~0.04 apfu pour des facteurs d'atomes O et Si ionisés à 0.25 apfu en adoptant des facteurs de dispersion pour les atomes O et Si neutres, illustration de l'importance de ces facteurs sur la quantité de $[^{14}\text{B}]$ qui est affinée. Un examen des distances $\langle T-\text{O} \rangle$ en fonction des rayons regroupés des cations dans les tourmalines contenant $[^{14}\text{B}]$ et $[^{27}\text{Al}]$ montre de grands écarts, et démontre la nécessité d'obtenir des données plus justes. Les limites de détection de $[^{11}\text{B}]$ et $[^{27}\text{Al}]$ dans une tourmaline par résonance magnétique nucléaire et spin à l'angle magique ont été étudiées avec des spectres simulés. Pour des teneurs minimales et maximales des métaux de transition (paramagnétiques), <0.04 et 0.12 apfu , les limites de détection du $[^{14}\text{B}]$ seraient entre ~0.02 et 0.08 apfu , et celles du $[^{14}\text{Al}]$, entre ~0.01 et 0.01 apfu , respectivement. La spectroscopie MAS NMR des isotopes $[^{11}\text{B}]$ et $[^{27}\text{Al}]$ n'appuient donc pas la présence de B ou Al en coordinence tétraédrique au delà du seuil de détection dans ces échantillons. Ces résultats concordent avec nos affinement reposant sur des facteurs de dispersion, ionisé dans le cas de O et pour un atome neutre dans le cas de Si, ce qui laisse croire que ce choix de courbes produit des résultats plus justes qu'un affinement avec seulement des facteurs pour atomes neutres. Les distances $\langle Z-\text{O} \rangle$ tombent dans l'intervalle 1.904–1.907 Å, avec une moyenne globale de 1.9047(8) Å, et l'affinement des structures indique des valeurs de dispersion aux sites en accord avec une occupation complète du site Z par Al. C'est donc dire que dans ce cristal zoné de façon complexe, Si est égal à 6.00 apfu , ainsi que $Z\text{Al}$.

(Traduit par la Rédaction)

Mots-clés: liddicoatite, elbaïte, tourmaline, zonation oscillatoire, affinement de la structure cristalline, analyse avec une microsonde électronique, résonance magnétique nucléaire avec spin à l'angle magique, spectroscopie de Mössbauer, populations des sites, Anjanabonoina, Madagascar.

INTRODUCTION

Liddicoatite, ideally $\text{Ca}(\text{Li}_2\text{Al})\text{Al}_6(\text{Si}_6\text{O}_{18})(\text{BO}_3)_3(\text{OH})_3\text{F}$ (Hawthorne & Henry 1999), is a calcic tourmaline occurring in late-stage mineral assemblages of rare-element elbaite-subtype pegmatites (see Dirlam *et al.* 2002, and references therein). It is a comparatively uncommon mineral, as the geological conditions required for the concentration of both Ca and Li are unusual; these elements typically show contrasting geochemical behavior in the later stages of pegmatite crystallization. Liddicoatite from Madagascar has long been known for its spectacular patterns of color zoning (Dunn *et al.* 1977, 1978). Although liddicoatite occurs at other localities (*e.g.*, Sahama *et al.* 1979, Zagorsky *et al.* 1989, Novák *et al.* 1999, Teertstra *et al.* 1999, Dirlam *et al.* 2002), crystals from these localities do not show the elaborate patterns of zoning that have made Malagasy liddicoatite a highly prized mineral with collectors.

Tourmaline is a useful petrogenetic indicator in granites and granitic pegmatites (Aurisicchio *et al.* 1999, Dyar *et al.* 1999, Novák & Povondra 1995, Novák *et al.* 1999, Selway *et al.* 1999, 2000a, 2000b, 2002, Agrosi *et al.* 2006, Neiva *et al.* 2007) and a wide variety of metamorphic rocks (Henry & Dutrow 1992, 1996, Henry & Guidotti 1985, Povondra & Novák 1986). There has been considerable work done on the characterization (*e.g.*, Hawthorne *et al.* 1993, MacDonald *et al.* 1993, Taylor *et al.* 1995, MacDonald & Hawthorne 1995, Dyar *et al.* 1998, Bosi 2008, Bosi & Lucchesi 2004, Bosi *et al.* 2004, 2005a, 2005b, Burns *et al.* 1994, Bloodaxe *et al.* 1999, Grice & Ercit 1993, Grice *et al.* 1993, Francis *et al.* 1999, Cámara *et al.* 2002, Schreyer *et al.* 2002, Ertl & Hughes 2002, Ertl *et al.* 2003a, 2003b, 2004, 2005, 2007, 2008, Hughes *et al.* 2000, 2004, Marschall *et al.* 2004, Andreozzi *et al.* 2008, Lussier *et al.* 2008a, 2008b, 2009) and

understanding (Hawthorne 1996, 2002, Pieczka 1999, Bosi 2008, Bosi & Lucchesi 2007) of site occupancy in tourmaline. Here, we characterize the compositional and structural aspects of oscillatory zoning in a single crystal of liddicoatite from its type locality, Anjanabonoina, central Madagascar, using Electron Micro-Probe Analysis (EMPA), crystal-Structure REFinement (SREF), Magic-Angle-Spinning Nuclear Magnetic Resonance (MAS NMR) spectroscopy and Mössbauer spectroscopy.

PROVENANCE

The pegmatites of central Madagascar were emplaced about 490 million years ago during late-stage granitic plutonism related to the Pan-African event, which occurred from 570 to 455 million years ago (Paquette & Nédélec 1998). These pegmatites are hosted by gneisses, marbles and quartzites of the Itremo Group, which overlies the crystalline basement of the Mozambique Orogenic Belt (Malisa & Muhongo 1990, Ashwal & Tucker 1999, Dissanayake & Chandrajith 1999, Collins & Windley 2002, Dirlam *et al.* 2002).

Although the crystal examined here is known to be from central Madagascar, we are not certain as to its exact locality; however, the Anjanabonoina pegmatite, located about 55 km west-southwest of the city of Antsirabe in Antananarivo Province, is famous for producing such crystals. In support of this provenance, the tourmaline section examined here (Fig. 1a) bears a very strong resemblance to the tourmaline from Anjanabonoina illustrated in Lacroix (1922, Fig. 329). According to the classification scheme of Černý (1982), this pegmatite is intermediate between the LCT and NYF families of the rare-element and miarolitic classes. The Anjanabonoina pegmatite is enriched in Na and Li, and has pronounced structural and mineralogical

internal zoning; it contains large miarolitic cavities, up to ~5 m in dimension, is heavily kaolinized by late-stage hydrothermal fluids, and consists of assemblages of quartz, feldspar, beryl, hambergite, danburite, phenakite and scapolite. Pezzotta (1996) reported the geologically most significant characteristics of the Anjanabonoina deposit to be (1) extremely high content of B, resulting in an abundance of tourmaline and primary danburite, and (2) the widespread presence of Ca, leading to the abundance of liddicoatite, danburite and diopside.

BIAXIAL OPTICS IN LIDDICOATITE

For over a century, tourmaline showing anomalous biaxiality has been reported (*e.g.*, Braun 1881,

Madelung 1883, Foord & Cunningham 1978, Foord & Mills 1978, Gorskaya *et al.* 1982, Akizuki *et al.* 2001, Shtukenberg *et al.* 2007). The origin of the anomalous optics has been debated for over two centuries (*e.g.*, Kahr & McBride 1992). However, it is now generally believed that the lowering of symmetry results from (1) ordering of atoms during growth owing to selective attachment of atoms to sites that are symmetrically equivalent in the bulk crystal but not at the growing crystal face (*e.g.*, Akizuki & Sunagawa 1978, Akizuki & Terada 1998, Akizuki *et al.* 1979), or (2) intrinsic stress as a result of compositional inhomogeneity in the crystal (*e.g.*, Gorskaya *et al.* 1982). Shtukenberg *et al.* (2007) examined in detail a prismatic crystal of elbaite-liddicoatite from the Malkhan pegmatite field

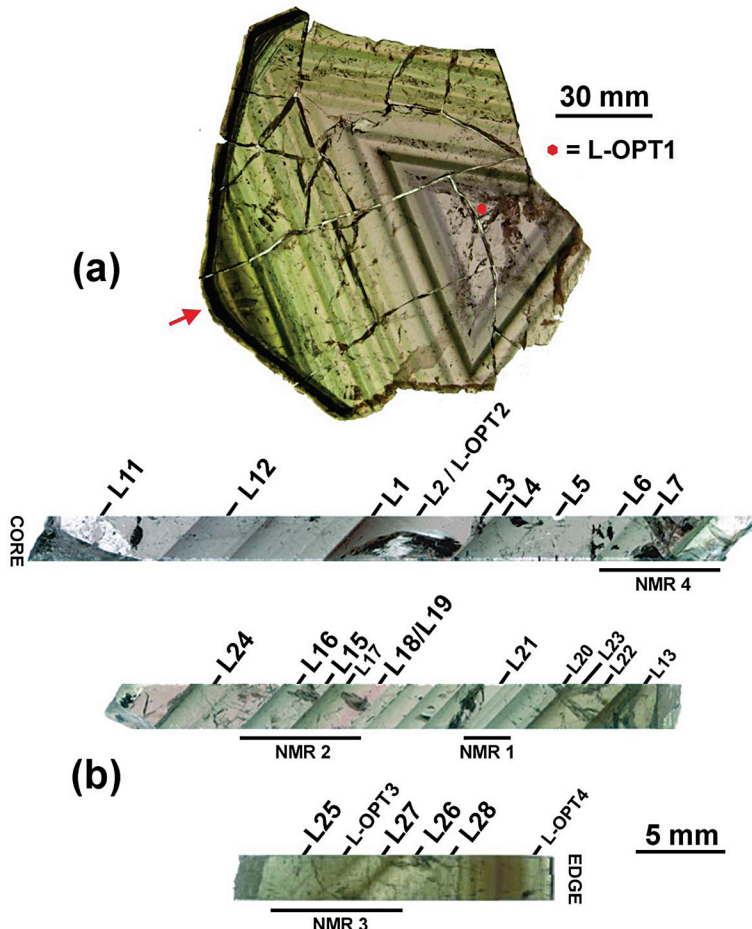


FIG. 1. The liddicoatite crystal investigated in this study: (a) slice perpendicular to the c axis showing oscillatory color zoning; (b) location of samples used for SREF, MAS NMR, and optical investigation along the strip of crystal extracted from the large crystal at the location of the red arrow.

in the Transbaikal region, Russia, consisting of the following growth sectors: $m\{10\bar{1}0\}$, $a\{11\bar{2}0\}$, $o\{02\bar{2}1\}$ and $r\{10\bar{1}1\}$. They measured the optic axial angle ($2V$) and collected single-crystal X-ray intensity data on three crystals from the $o\{02\bar{2}1\}$ growth sector with $2V$ values of $11(1)$, $16(1)$ and $23(1)^\circ$, respectively. They collected a complete Ewald sphere of intensity data on each of these three crystals and reported a significant decrease in $R(\text{int})$ values if reflection data were merged in the monoclinic space-group Cm [$R(\text{int}) = 1.86\text{--}3.15\%$] as opposed to the trigonal space group $R3m$ [$R(\text{int}) = 5.04\text{--}7.24\%$]. Moreover, $\sim 20\text{--}40\%$ of reflections violate the requirements of the 3 and m_i symmetry operators, but not the m_y symmetry operator, suggesting monoclinic symmetry. The R indices for their refinement in $R3m$, Cm and $R1$ are $2.20\text{--}2.70$, $1.86\text{--}2.55$ and $1.97\text{--}2.81\%$, respectively, and refining the structures in either monoclinic (Cm) or triclinic ($R1$) symmetries gave a direct correlation between the degree of order at the Y sites and the corresponding $2V$ angles.

EXPERIMENTAL

The liddicoatite specimen used in this study was obtained from the Harvard Mineralogical Museum. It is a slice ~ 5 -mm thick (Fig. 1), cut perpendicular to the c axis through the pyramidal zoning section of a much larger crystal, the exact dimensions of which are unknown. There are four major divisions in color (from core to edge): (1) purple (~ 5 cm wide); (2) pale green (~ 5 cm wide); (3) dark green (~ 2 cm wide); (4) dark green-black (~ 0.7 cm wide). Each of these major color divisions consists of many smaller zones (Fig. 1), which are distinguished by the oscillatory repetition of diffuse color variations, and bordered by sharp, grayish green to black boundaries, each of which is inclined at $\sim 45^\circ$ to the (001) plane. Near the edge of the crystal, the form of the zones becomes prismatic and sharp as opposed to diffuse.

Samples were extracted from the main crystal at four different positions (Fig. 1), and the $2V$ angles were measured with a spindle stage and the program EXCALIBR II (Bartelmehs *et al.* 1992). Sample L-OPT1, taken from the purple center of the crystal, has uniaxial optics ($2V = 0.0^\circ$); samples L-OPT2 and L-OPT3, taken from the pyramidal zone, have $2V$ values of $8(3)$ and $18.9(5)^\circ$, respectively, and L-OPT4, taken from the prism zone, has a $2V$ value of $20.5(9)^\circ$.

Collection of X-ray data

Twenty-three small fragments were extracted, ground to (approximate) spheres and mounted on a Bruker P3 automated four-circle single-crystal diffractometer equipped with a serial detector and a graphite-monochromated $MoK\alpha$ X-radiation source. Cell dimensions (Table 1) were derived from the setting angles of thirteen automatically aligned reflections by

least-squares refinement. A total of ~ 1110 symmetry-independent reflections was measured for each crystal over the interval $4^\circ < 2\theta < 60^\circ$, with index ranges $0 < h < 23$, $0 < k < 23$, $-11 < l < 11$. A standard reflection was collected every 50 measurements to monitor instrument stability; no significant change was noted during any of the data collections. Psi-scan intensity data were collected, a psi-scan absorption correction was applied to each crystal, together with the usual geometrical corrections, and the data were reduced to structure factors. Additional details of the data collection and refinement are given in Table 1.

Space group

X-ray intensity data were collected on crystals denoted here as L-OPT1–4 (with $2V$ values corresponding to those measured above) using an APEX CCD detector. In excess of a hemisphere of data was collected for each crystal in order to test for diffraction symmetry (Table 2). The calculated $R(\text{int})$ values for L-OPT1–3 with trigonal symmetry are 1.73 , 2.41 and 1.99% , respectively, and with monoclinic symmetry are 1.38 , 1.88 and 1.67% , an insignificant difference. Shtukenberg *et al.* (2007) found that cation order at the three edge-sharing Y octahedra resulted in poor $R(\text{int})$ values about two of the three mirror planes. We tested this issue for our three samples: The $R(\text{int})$ values for groups of reflections directly related by each of the three mirror planes at $(x\ 2z)$, $(2x\ xz)$ and $(x-xz)$ were calculated. The results (Table 2) indicate no difference in merge quality for any particular mirror, and all values of $R(\text{int})$ are $< 1\%$. These results provide no evidence of lower symmetry in the diffraction data, and hence all structures were refined with $R3m$ symmetry.

Crystal-structure refinement

Crystal-structure refinement was done using the SHELXTL PLUS[®] (PC version) software package. All structures were refined with full occupancy of the Z site by Al and the B site by B in the space group $R3m$. All samples were refined twice, once with the O(1) site at $(0,0,z)$ and the O(2) site at $(x,1-x,z)$, and again with O(1) at $(x,2x,z)$ and O(2) at (x,y,z) to allow for positional disorder, as indicated by the high U_{eq} values (Burns *et al.* 1994). The final refinement was done with neutral scattering factors for all species except O, for which we used a fully ionized scattering factor (this procedure will be discussed in detail in the Results section). Each specimen was tested for absolute orientation and transformed as appropriate. An isotropic extinction correction of the form $k[1 + 0.001x F_c^2 \lambda^3 / \sin 2\theta]^{-1/4}$ was applied, and the values of x were in the range $0.0005(2)$ to $0.0060(3)$. The highest positive and negative residual electron-densities in final difference-Fourier maps were ~ 0.5 e \AA^{-3} at ~ 0.5 \AA from O(1), associated with minor problems modeling the

TABLE 1. DATA COLLECTION AND STRUCTURE-REFINEMENT INFORMATION
FOR SAMPLES OF LIDDICOATITE FROM MADAGASCAR

	L1	L2	L4	L5	L6	L7	L11	L12
a (Å)	15.8636(16)	15.8529(13)	15.8548(14)	15.8456(12)	15.8418(17)	15.8363(15)	15.8675(13)	15.853(7)
c (Å)	7.1119(9)	7.1101(8)	7.1099(8)	7.1066(7)	7.1044(10)	7.1040(9)	7.1135(8)	7.120(4)
V (Å ³)	1551.2(4)	1547.4(3)	1547.9(3)	1545.2(3)	1544.0(4)	1543.0(3)	1551.1(3)	1549.0(1)
Color	Dark pink	Pink	Pink	Pink	Pink	Pink	Pink	Pink
Unique	1111	1111	1111	1111	1111	1111	1111	1111
F _o > 4σ	1087	1092	1087	1088	1090	1096	1102	1095
R ₁ (obs.) %	1.77	1.66	1.80	1.70	1.71	1.64	1.73	1.73
wR ₂ (%)	4.43	4.32	4.45	4.27	4.29	4.11	4.41	4.27
GOOF	1.072	1.072	1.052	1.085	1.083	1.103	1.073	1.065
EXTI*	0.0042(3)	0.0025(2)	0.0028(2)	0.0037(3)	0.0026(2)	0.0037(3)	0.0020(2)	0.0046(3)
°R ₁ / °wR ₂ (%)**	1.90 / 4.75	1.85 / 4.71	1.94 / 4.66	1.73 / 4.29	1.80 / 4.43	1.75 / 4.30	1.94 / 4.80	1.92 / 4.77
	L13	L15	L16	L17	L18	L19	L20	L21
a (Å)	15.8449(15)	15.8248(16)	15.8307(10)	15.8337(12)	15.8293(11)	15.8343(11)	15.8303(11)	15.8399(11)
c (Å)	7.1053(9)	7.0993(9)	7.1013(6)	7.1023(7)	7.1003(6)	7.1012(7)	7.1017(6)	7.1030(6)
V (Å ³)	1544.9(3)	1539.6(4)	1541.3(2)	1541.9(3)	1540.7(3)	1541.8(3)	1541.2(3)	1543.5(5)
Color	Green	Dark green						
Unique	1111	1109	1109	1109	1109	1109	1109	1111
F _o > 4σ	1099	1097	1099	1088	1094	1094	1091	1104
R ₁ (obs.) %	1.96	2.23	1.44	1.62	1.61	1.69	1.70	1.68
wR ₂ (%)	4.84	5.89	3.75	4.03	4.09	4.29	4.10	6.03
GOOF	1.099	1.108	1.117	1.071	1.111	1.103	1.104	1.574
EXTI*	0.0026(2)	0.0039(4)	0.0052(3)	0.0034(2)	0.0034(3)	0.0061(3)	0.0034(2)	0.0036(3)
°R ₁ / °wR ₂ (%)**	2.05 / 5.03	2.32 / 6.11	1.51 / 3.78	1.67 / 4.00	1.72 / 4.31	1.77 / 4.46	1.80 / 4.28	1.87 / 5.05
	L22	L23	L24	L25	L26	L27	L28	
a (Å)	15.8306(16)	15.8299(13)	15.8286(14)	15.8438(14)	15.8368(11)	15.8333(14)	15.8404(13)	
c (Å)	7.0999(9)	7.1009(7)	7.1012(8)	7.1043(8)	7.1014(6)	7.1025(8)	7.1039(7)	
V (Å ³)	1540.9(4)	1540.9(3)	1540.9(3)	1544.4(3)	1542.4(2)	1541.8(3)	1543.6(3)	
Color	Green	Green	Green	Dark green	Dark green	Dark green	Dark green	
Unique	1109	1109	1109	1111	1109	1109	1111	
F _o > 4σ	1087	1098	1089	1096	1078	1086	1092	
R ₁ (obs.) %	2.95	1.51	1.58	1.83	1.81	1.71	1.54	
wR ₂ (%)	7.16	3.96	4.05	4.88	4.62	4.37	3.93	
GOOF	1.070	1.125	1.079	1.096	1.046	1.081	1.092	
EXTI*	0.0047(6)	0.0061(3)	0.0400(3)	0.0015(3)	0.0013(2)	0.0007(2)	0.0054(3)	
°R ₁ / °wR ₂ (%)**	2.95 / 7.32	1.64 / 4.27	1.68 / 4.18	1.98 / 5.17	1.88 / 4.60	1.83 / 4.56	1.69 / 4.24	

Space group, R3m; Z = 3; Radiation / monochromator: MoKa/graphite. All crystals were ~150–200 μm ground spheres.

* Maximizes agreement between F_o and F_ck [1 + (EXTI) F_c² λ³ / 10³ in (2θ)]^{-1/2}.

** With O(1) and O(2) constrained to (0, 0, z) and (x, -x, z), respectively.

positional disorder of the anion at O(1), and ~0.3 eÅ⁻³ at ~0.25 Å from H(3), associated with delocalization of electron density along the O(3)–H(3) bond, which was constrained to be close to 0.98 Å during refinement to give good interatomic distances involving H(3). The highest correlations in the refinements were of the order of ~0.84 and involved either the z coordinates of the T and Z sites or the x and y coordinates of the O(2)

site. Final R₁ and wR₂ indices are 1.48–2.97% (<R₁> = 1.78%) and 3.87–7.37 (<wR₂> = 4.71%), respectively (Table 1) for all observed reflections. Atom coordinates and selected interatomic distances of selected samples are given in Tables 3 and 4, respectively; refined site-scattering values (Hawthorne *et al.* 1995) are given in Table 5. Structure factors for all structures may be obtained from the Depository of Unpublished Data on

the Mineralogical Association of Canada website [document Liddicoatite CM49_63].

Electron-microprobe analysis

All crystals used for the collection of X-ray intensity data, and crystals from the samples used for MAS NMR spectroscopy, were analyzed with a Cameca SX-100 electron microprobe operating in wavelength-dispersion mode with an accelerating voltage of 20 kV, a specimen current of 15 nA, and a beam diameter of 10 μm . The following analyzing crystals and standards were used: TAP: albite (Na); andalusite (Al); diopside (Si); LPET: orthoclase (K); diopside (Ca); titanite (Ti); PbTe (Pb); LTAP: fluororiebeckite (F); forsterite (Mg); LLiF: fayalite (Fe); spessartine (Mn). The data were reduced and corrected by the PAP method of Pouchou & Pichoir (1985). Table 6 gives the chemical compositions (mean of ten determinations) and unit formulae calculated with the following assumptions, using the $\text{Fe}^{3+} / (\text{Fe}^{2+} + \text{Fe}^{3+})$ values determined by Mössbauer spectroscopy: 31 anions, $\text{OH} + \text{F} = 4 \text{ apfu}$ [in accord with the incident bond-valence sums at O(1) and O(3)], $\text{B} = 3 \text{ apfu}$, ${}^7\text{Al} = 6 \text{ apfu}$; all Mn is assumed to be divalent as not all Fe is trivalent, and $\text{Li} = (3 - \Sigma Y) \text{ apfu}$. The normalization scheme was iterated to self-consistency.

Magic-angle-spinning nuclear magnetic resonance spectroscopy

A Varian Inova[®] 600 spectrometer (14.1 T) was used to record the MAS NMR spectra of ${}^{27}\text{Al}$ ($\nu_L = 156.3 \text{ MHz}$) and ${}^{11}\text{B}$ ($\nu_L = 194.2 \text{ MHz}$) in four samples; these are labeled NMR1–NMR4, and their location on the sample is shown in Figure 1. For each sample, a weighed amount (~30 mg) of powdered sample (~15 μm crystallites) was placed in a 3.2 mm (22 μL capacity) zirconia rotor and spun at spinning speeds of $18 - 24 \pm 0.003 \text{ kHz}$ in a double-resonance probe. The optimized recycle delay was determined independently for each sample; averages were 7 and 5 s for ${}^{27}\text{Al}$ and ${}^{11}\text{B}$, respectively. The final spectra are composites of 512–3072 averaged scans. Spectra were referenced to 0.1 M H_3BO_3 as a secondary reference [$\delta = +19.6 \text{ ppm}$ with respect to $\text{BF}_3(\text{CH}_3\text{CH}_2)_2\text{O}$], and 0.1 M $\text{Al}(\text{NO}_3)_3$. Pulse widths were selected to coincide approximately with a 15° tip angle at an rf nutation frequency of 42 kHz (${}^{11}\text{B}$) and 52 kHz (${}^{27}\text{Al}$). A spectrum was collected on each empty rotor prior to sample packing to rule out cross-contamination and spectral interference from rotor materials. A Bruker Avance II 900 (21.1 T) spectrometer was used to record the ${}^{27}\text{Al}$ ($\nu_L = 234.4 \text{ MHz}$) MAS NMR spectrum of sample NMR2. A 1.3 mm ZrO_2 rotor was spun at $62.000 \pm 0.002 \text{ kHz}$, and acquired with a 12° tip angle ($\nu_{rf} = 73 \text{ kHz}$), a recycle delay of 5 s and 1024 co-added transients.

${}^{57}\text{Fe}$ Mössbauer spectroscopy

The Fe content of this crystal is quite low, averaging considerably less than 1 wt% FeO, and as a result, we could not measure Mössbauer spectra for each color zone. Instead, we measured spectra on aggregate samples from the pyramidal and prismatic sectors to give us some basis for treating Fe in the calculation of the unit formulae. Powdered samples from the pyramidal and prismatic zones were mixed with sucrose and carefully ground under acetone. The mixtures were loaded into Pb rings (2 mm inner diameter) and covered by tape on both sides. Mössbauer spectra were acquired at room temperature in transmission geometry using a ${}^{57}\text{Co}(\text{Rh})$ point source. The spectrometer was calibrated with the room-temperature spectrum of $\alpha\text{-Fe}$. The spectra were fit by Lorentzian doublets method using the RECOIL[®] software package; fitting parameters are given in Table 7.

RESULTS

MAS NMR spectroscopy

Magic-angle spinning NMR is sensitive to the coordination number of ${}^{11}\text{B}$ (Bray *et al.* 1961, Turner *et al.* 1986) and ${}^{27}\text{Al}$ (Kirkpatrick 1988, Kirkpatrick *et al.* 1985, 1986). Chemical shifts of [4]- and [3]-coordinated B, and [4]- and [6]-coordinated Al, in tourmaline are well-resolved in MAS NMR spectra (e.g., Tagg *et al.* 1999, Schreyer *et al.* 2002, Marler & Ertl 2002, Lussier *et al.* 2008a, 2009). For both nuclei, MAS NMR can be used to detect the presence of very small amounts of [4]-coordinated species in the presence of much greater amounts of [3]- and [6]-coordinated B and Al, respectively. The ${}^{11}\text{B}$ and ${}^{27}\text{Al}$ MAS NMR spectra are presented in Figures 2 and 3, respectively. In all spectra, only one peak is observed. These spectra clearly lack any observable intensity in the regions characteristic for tetrahedrally coordinated species (~0 ppm for B; 50–70 ppm for Al). There is the suggestion of a shoulder at ~0 ppm in Figure 2b, and the simulated spectra of

TABLE 2. CALCULATED $R(\text{int})$ VALUES* FOR LIDDICOATITE ACROSS $R3m$ MIRROR PLANES

		$x, 2x, z$	$2x, x, z$	$x, -x, z$
L-OPT1	$R(\text{int}) * (\%)$	2.57	2.54	2.45
	N	2138	2167	2078
L-OPT2	$R(\text{int})$	4.53	4.43	4.51
	N	1991	2076	2006
L-OPT3	$R(\text{int})$	3.22	3.08	3.08
	N	2107	2138	2094
L-OPT4	$R(\text{int})$	4.32	4.39	4.51
	N	2245	2165	2116

* averages calculated using $\sum |F_o|^2 - \langle F_o^2 \rangle | / \sum |F_o|^2$ on N pairs of reflections.

TABLE 3. FINAL POSITIONS* AND EQUIVALENT ISOTROPIC-DISPLACEMENT PARAMETERS (\AA^2) OF ATOMS IN CRYSTALS OF LIDDICOATITE

		L1	L2	L4	L5	L6	L7	L11	L12
X	x	0	0	0	0	0	0	0	0
	y	0	0	0	0	0	0	0	0
	z	0.76101(17)	0.76028(14)	0.76060(17)	0.76011(15)	0.76028(15)	0.76057(14)	0.76038(16)	0.76015(15)
Y	U_{eq}	0.0175(3)	0.0157(3)	0.0165(3)	0.0143(3)	0.0145(3)	0.0144(3)	0.0173(3)	0.01604
	x	0.06192(4)	0.06195(4)	0.06191(4)	0.06192(4)	0.06188(4)	0.06185(4)	0.06200(3)	0.06192(4)
Z	y	0.93808(4)	0.93805(4)	0.93809(4)	0.93808(4)	0.93812(4)	0.93815(4)	0.93800(3)	0.93808(4)
	z	0.36906(15)	0.36814(15)	0.36813(16)	0.36673(17)	0.36596(18)	0.36575(16)	0.37036(14)	0.36940(15)
	U_{eq}	0.0113(3)	0.0117(3)	0.0114(3)	0.0117(4)	0.0124(4)	0.0113(3)	0.0108(3)	0.0115(3)
T	x	0.26015(4)	0.25992(3)	0.26002(4)	0.25977(4)	0.25972(4)	0.25973(3)	0.26026(4)	0.26009(4)
	y	0.29717(4)	0.29700(3)	0.29703(4)	0.29691(3)	0.29686(3)	0.29683(3)	0.29728(3)	0.29709(3)
	z	0.38793(10)	0.38782(9)	0.38784(10)	0.38791(9)	0.38801(9)	0.38801(9)	0.38757(9)	0.38774(9)
B	U_{eq}	0.00617(11)	0.00640(10)	0.00647(11)	0.00637(11)	0.00633(11)	0.00640(10)	0.00609(11)	0.00653(10)
	x	0.19025(3)	0.19020(3)	0.19018(3)	0.19025(3)	0.19023(3)	0.19017(3)	0.19021(3)	0.19020(3)
O(1) ^d	y	0.19213(3)	0.19215(3)	0.19210(3)	0.19215(3)	0.19212(3)	0.19210(3)	0.19214(3)	0.19212(2)
	z	0	0	0	0	0	0	0	0
	U_{eq}	0.00496(10)	0.00507(9)	0.00515(10)	0.00511(9)	0.00500(9)	0.00518(9)	0.00493(9)	0.00518(9)
O(1) ^o	x	0.89084(10)	0.89089(9)	0.89101(10)	0.89099(10)	0.89104(10)	0.89115(9)	0.89067(10)	0.89096(9)
	y	0.10916(10)	0.10911(9)	0.10899(10)	0.10901(10)	0.10896(10)	0.10885(9)	0.10933(10)	0.10904(9)
	z	0.54483(3)	0.54513(3)	0.54484(4)	0.54463(3)	0.54473(3)	0.54443(3)	0.54513(3)	0.54543(3)
O(2) ^d	U_{eq}	0.00641(4)	0.0068(4)	0.0072(4)	0.0075(4)	0.0068(4)	0.0069(4)	0.0069(4)	0.0069(4)
	x	0.01155(15)	0.01152(13)	0.01134(15)	0.01136(15)	0.01128(15)	0.01111(14)	0.01214(13)	0.01165(13)
	y	0.02313(3)	0.0230(3)	0.0227(3)	0.0227(3)	0.0226(3)	0.0222(3)	0.0243(3)	0.0233(3)
O(2) ^o	z	0.2115(5)	0.2118(5)	0.2125(5)	0.2119(5)	0.2114(5)	0.2117(5)	0.2112(5)	0.2111(5)
	U_{eq}	0.0149(11)	0.014(1)	0.0144(11)	0.0151(11)	0.0145(11)	0.014(1)	0.014(1)	0.012(1)
	x	0	0	0	0	0	0	0	0
O(3)	y	0	0	0	0	0	0	0	0
	z	0.2117(6)	0.2120(5)	0.2126(5)	0.2121(5)	0.2115(5)	0.2118(5)	0.2114(6)	0.2113(6)
	U_{eq}	0.0566(14)	0.0554(13)	0.0537(13)	0.0551(13)	0.0540(13)	0.0522(12)	0.0612(16)	0.0549(14)
O(4)	x	0.9302(2)	0.9304(2)	0.9308(2)	0.9305(2)	0.9306(2)	0.9309(2)	0.9298(2)	0.9300(2)
	y	0.0508(2)	0.0505(2)	0.0511(2)	0.0509(2)	0.0509(2)	0.0510(2)	0.0507(2)	0.0505(2)
	z	0.5200(3)	0.5197(3)	0.5195(3)	0.5196(3)	0.5196(3)	0.5197(2)	0.5207(3)	0.5202(3)
O(5)	U_{eq}	0.0087(5)	0.0102(5)	0.0088(5)	0.0088(5)	0.0092(5)	0.0095(4)	0.0090(5)	0.0088(4)
	x	0.93974(7)	0.93998(7)	0.93983(7)	0.93986(7)	0.93990(7)	0.94001(7)	0.93960(7)	0.93979(7)
	y	0.06026(7)	0.06002(7)	0.06017(7)	0.06014(7)	0.06010(7)	0.05999(7)	0.06040(7)	0.06021(7)
O(6)	z	0.5202(4)	0.5199(3)	0.5197(3)	0.5198(3)	0.5198(3)	0.5199(3)	0.5209(3)	0.5203(3)
	U_{eq}	0.0171(5)	0.0183(5)	0.0162(5)	0.0167(4)	0.0171(4)	0.0169(4)	0.0180(5)	0.0176(5)
	x	0.13483(7)	0.13490(7)	0.13478(7)	0.13478(7)	0.13493(7)	0.13484(7)	0.13504(7)	0.13492(7)
O(7)	y	0.86517(7)	0.86510(7)	0.86522(7)	0.86522(7)	0.86507(7)	0.86516(7)	0.86496(7)	0.86508(7)
	z	0.4897(2)	0.4893(2)	0.4895(2)	0.4895(2)	0.4899(2)	0.4896(2)	0.4894(2)	0.4894(2)
	U_{eq}	0.0100(3)	0.0102(3)	0.0101(4)	0.0104(3)	0.0103(3)	0.0104(3)	0.0091(3)	0.0102(3)
O(8)	x	0.90771(7)	0.90773(6)	0.90773(7)	0.90781(7)	0.90780(6)	0.90786(6)	0.90755(6)	0.90767(6)
	y	0.09229(7)	0.09227(6)	0.09227(7)	0.09219(7)	0.09220(6)	0.09214(6)	0.09245(6)	0.09233(6)
	z	0.9269(2)	0.9263(2)	0.9265(2)	0.9255(2)	0.9256(2)	0.9257(2)	0.9268(2)	0.9268(2)
O(9)	U_{eq}	0.00803(3)	0.0081(3)	0.0082(3)	0.0087(3)	0.0084(3)	0.0085(3)	0.0078(3)	0.0085(3)
	x	0.09234(7)	0.09213(6)	0.09226(7)	0.09217(7)	0.09210(7)	0.09203(6)	0.09244(7)	0.09227(6)
	y	0.90766(7)	0.90787(6)	0.90774(7)	0.90783(7)	0.90790(7)	0.90797(6)	0.90756(7)	0.90773(6)
O(10)	z	0.9054(2)	0.9047(2)	0.9048(2)	0.9041(2)	0.9042(2)	0.9042(2)	0.9053(2)	0.9051(2)
	U_{eq}	0.00823(3)	0.0086(3)	0.0090(3)	0.0082(3)	0.0085(3)	0.0084(3)	0.0081(3)	0.0088(3)
	x	0.18672(8)	0.18644(8)	0.18634(8)	0.18640(8)	0.18632(8)	0.18607(8)	0.18694(8)	0.18674(8)
O(11)	y	0.19640(8)	0.19624(8)	0.19616(8)	0.19590(8)	0.19597(8)	0.19593(8)	0.19657(8)	0.19646(8)
	z	0.22361(17)	0.22358(16)	0.22358(18)	0.22349(17)	0.22365(17)	0.22357(16)	0.22355(17)	0.22354(16)
	U_{eq}	0.0074(2)	0.0074(2)	0.0074(2)	0.0071(2)	0.0071(2)	0.0071(2)	0.0073(2)	0.0073(2)
O(12)	x	0.28551(8)	0.28547(7)	0.28554(8)	0.28537(8)	0.28534(8)	0.28541(7)	0.28546(8)	0.28551(7)
	y	0.28578(8)	0.28581(8)	0.28588(8)	0.28589(8)	0.28596(8)	0.28596(8)	0.28565(8)	0.28579(8)
	z	0.91842(16)	0.91820(15)	0.91854(16)	0.91828(16)	0.91837(16)	0.91831(15)	0.91811(16)	0.91824(15)
O(13)	U_{eq}	0.0063(2)	0.0063(2)	0.0064(2)	0.0064(2)	0.0064(2)	0.0065(2)	0.0062(2)	0.0064(2)
	x	0.27012(9)	0.27016(8)	0.27019(9)	0.27004(9)	0.27000(9)	0.26996(8)	0.27017(9)	0.27016(9)
	y	0.20968(9)	0.20953(8)	0.20964(9)	0.20972(9)	0.20969(9)	0.20947(8)	0.20974(8)	0.20967(8)
O(14)	z	0.55784(17)	0.55771(16)	0.55767(17)	0.55772(16)	0.55794(17)	0.55779(15)	0.55749(17)	0.55772(16)
	U_{eq}	0.0075(2)	0.0077(2)	0.0076(2)	0.0075(2)	0.0076(2)	0.0074(2)	0.0076(2)	0.0082(2)
	x	0.1337(12)	0.130(2)	0.1303(12)	0.1321(12)	0.1306(12)	0.1279(12)	0.1319(12)	0.1311(12)
H(3)	y	0.8663(12)	0.870(2)	0.8697(12)	0.8679(12)	0.8694(12)	0.8721(12)	0.8681(12)	0.8689(12)
	z	0.624(3)	0.6256(13)	0.625(3)	0.623(3)	0.622(3)	0.620(3)	0.623(3)	0.624(3)
	U_{eq}	0.015	0.015	0.015	0.015	0.015	0.015	0.015	0.015

* The superscripts o and d on O(1) and O(2) denote the ordered and disordered atom coordinates for these sites.

** Fixed during the refinement.

TABLE 3 (cont'd). FINAL POSITIONS* AND EQUIVALENT ISOTROPIC-DISPLACEMENT PARAMETERS (\AA^2) OF ATOMS IN CRYSTALS OF LIDDOCOATITE

		L13	L15	L16	L17	L18	L19	L20	L21
X	x	0	0	0	0	0	0	0	0
	y	0	0	0	0	0	0	0	0
	z	0.76231(19)	0.76133(17)	0.76121(12)	0.76167(14)	0.76118(14)	0.76142(14)	0.76161(15)	0.76207(15)
Y	U_{eq}	0.0161(4)	0.0134(3)	0.0142(2)	0.0148(3)	0.0140(3)	0.0141(3)	0.0136(3)	0.0147(3)
	x	0.06196(5)	0.06182(6)	0.06184(4)	0.06183(4)	0.06182(4)	0.06186(4)	0.06175(5)	0.06183(4)
	y	0.93804(5)	0.93818(6)	0.93816(4)	0.93817(4)	0.93818(4)	0.93814(4)	0.93825(5)	0.93817(4)
Z	z	0.36590(19)	0.3637(2)	0.36437(16)	0.36458(17)	0.36366(18)	0.36396(18)	0.36394(19)	0.36477(17)
	U_{eq}	0.0110(4)	0.0113(5)	0.0103(3)	0.0110(3)	0.0110(4)	0.0110(4)	0.0103(4)	0.0105(4)
	x	0.25978(4)	0.25956(4)	0.25959(3)	0.25965(3)	0.25957(3)	0.25958(3)	0.25959(4)	0.25969(3)
T	y	0.29699(4)	0.29670(4)	0.29671(3)	0.29678(3)	0.29670(3)	0.29672(3)	0.29668(3)	0.29684(3)
	z	0.38818(11)	0.38834(11)	0.38825(8)	0.38821(9)	0.38821(9)	0.38819(9)	0.38827(9)	0.38829(9)
	U_{eq}	0.00631(12)	0.00608(13)	0.00608(9)	0.00616(10)	0.00626(10)	0.00609(10)	0.00590(10)	0.00592(10)
B	x	0.19019(4)	0.19020(3)	0.19018(3)	0.19020(3)	0.19018(3)	0.19019(3)	0.19017(3)	0.19020(3)
	y	0.19212(3)	0.19210(3)	0.19206(2)	0.19211(3)	0.19211(3)	0.19210(3)	0.19207(3)	0.19212(3)
	z	0	0	0	0	0	0	0	0
O(1) ^d	U_{eq}	0.00539(11)	0.00509(12)	0.00493(8)	0.00530(9)	0.00528(9)	0.00509(9)	0.00471(9)	0.00494(9)
	x	0.89082(11)	0.89111(11)	0.89126(8)	0.89120(9)	0.89123(9)	0.89106(9)	0.89135(10)	0.89109(10)
	y	0.10918(11)	0.10889(11)	0.10874(8)	0.10880(9)	0.10877(9)	0.10894(9)	0.10865(10)	0.10891(10)
O(1) ^o	z	0.5450(4)	0.5446(4)	0.5447(3)	0.5444(3)	0.5444(3)	0.5447(3)	0.5448(3)	0.5449(3)
	U_{eq}	0.0073(5)	0.0067(5)	0.0068(3)	0.0071(4)	0.0069(4)	0.0069(4)	0.0070(4)	0.0068(4)
	x	0.01115(17)	0.01091(17)	0.01085(12)	0.01108(14)	0.01073(14)	0.01096(14)	0.01078(15)	0.01101(15)
O(2) ^d	y	0.0223(4)	0.0218(3)	0.0217(2)	0.0222(3)	0.0215(3)	0.0219(3)	0.0216(3)	0.0220(3)
	z	0.2128(6)	0.2114(6)	0.2115(4)	0.2120(5)	0.2108(4)	0.2114(5)	0.2114(5)	0.2119(5)
	U_{eq}	0.0158(12)	0.0148(12)	0.0131(9)	0.015(1)	0.013(1)	0.014(1)	0.0138(11)	0.0152(11)
O(2) ^o	x	0	0	0	0	0	0	0	0
	y	0	0	0	0	0	0	0	0
	z	0.2130(6)	0.2116(7)	0.2117(5)	0.2121(5)	0.2110(5)	0.2115(5)	0.2117(5)	0.2123(7)
O(3)	U_{eq}	0.0546(15)	0.0522(15)	0.0492(10)	0.0521(12)	0.0482(11)	0.0518(12)	0.0491(12)	0.0535(15)
	x	0.9306(3)	0.93061(2)	0.93127(19)	0.9311(2)	0.9313(2)	0.9311(2)	0.9314(2)	0.9307(2)
	y	0.0511(3)	0.0506(2)	0.05097(19)	0.0511(2)	0.0511(2)	0.0510(2)	0.0510(2)	0.0509(2)
O(4)	z	0.5190(3)	0.5188(3)	0.5194(2)	0.5187(2)	0.5191(2)	0.5190(2)	0.5191(3)	0.5190(3)
	U_{eq}	0.0090(5)	0.0082(5)	0.0093(4)	0.0091(4)	0.0092(4)	0.0089(4)	0.0086(5)	0.0089(5)
	x	0.93980(8)	0.94007(8)	0.94020(6)	0.94006(7)	0.94015(7)	0.94010(7)	0.94025(7)	0.94008(8)
O(5)	y	0.06020(8)	0.05993(8)	0.05980(6)	0.05994(7)	0.05985(7)	0.05990(7)	0.05975(7)	0.05992(8)
	z	0.5191(4)	0.5188(4)	0.5197(3)	0.5189(3)	0.5193(3)	0.5190(3)	0.5193(3)	0.5195(3)
	U_{eq}	0.0167(5)	0.0164(5)	0.0164(4)	0.0162(4)	0.0161(4)	0.0162(4)	0.0157(4)	0.0168(5)
O(6)	x	0.13458(8)	0.13465(8)	0.13462(6)	0.13461(7)	0.13448(7)	0.13455(7)	0.13470(7)	0.13454(7)
	y	0.86542(8)	0.86535(8)	0.86538(6)	0.86539(7)	0.86552(7)	0.86545(7)	0.86530(7)	0.86546(7)
	z	0.4900(3)	0.4902(3)	0.48995(19)	0.4899(2)	0.4899(2)	0.4899(2)	0.4902(2)	0.4900(2)
O(7)	U_{eq}	0.0100(4)	0.0105(4)	0.0107(3)	0.0106(3)	0.0111(3)	0.0105(3)	0.0104(3)	0.0102(3)
	x	0.90765(7)	0.90785(8)	0.90791(5)	0.90785(6)	0.90791(6)	0.90793(6)	0.90792(6)	0.90782(6)
	y	0.09235(7)	0.09215(8)	0.09209(5)	0.09215(6)	0.09209(6)	0.09207(6)	0.09208(6)	0.09218(6)
O(8)	z	0.9255(3)	0.9248(3)	0.92522(19)	0.9253(2)	0.9252(2)	0.9248(2)	0.9252(2)	0.9257(2)
	U_{eq}	0.0085(4)	0.0084(4)	0.0084(3)	0.0084(3)	0.0083(3)	0.0081(3)	0.0077(3)	0.0080(3)
	x	0.09219(8)	0.09192(8)	0.09198(6)	0.09199(6)	0.09197(6)	0.09207(6)	0.09194(7)	0.09204(7)
H(3)	y	0.90781(8)	0.90808(8)	0.90802(6)	0.90801(6)	0.90803(6)	0.90793(6)	0.90806(7)	0.90796(7)
	z	0.9043(3)	0.9042(3)	0.90386(19)	0.9039(2)	0.9037(2)	0.9040(2)	0.9037(2)	0.9041(2)
	U_{eq}	0.0085(3)	0.0079(3)	0.0083(3)	0.0088(3)	0.0085(3)	0.0083(3)	0.0078(3)	0.0086(3)
O(9)	x	0.18640(10)	0.18579(10)	0.18587(7)	0.18605(8)	0.18598(8)	0.18595(8)	0.18585(8)	0.18617(8)
	y	0.19593(9)	0.19537(9)	0.19569(7)	0.19576(8)	0.19565(7)	0.19554(8)	0.19565(8)	0.19579(8)
	z	0.22381(19)	0.22233(2)	0.22358(14)	0.22368(16)	0.22373(16)	0.22357(16)	0.22351(17)	0.22380(17)
O(10)	U_{eq}	0.0073(2)	0.0072(3)	0.00718(18)	0.0072(2)	0.0075(2)	0.0070(2)	0.0068(2)	0.0071(2)
	x	0.28531(9)	0.28522(9)	0.28539(6)	0.28538(7)	0.28547(7)	0.28524(7)	0.28545(8)	0.28527(8)
	y	0.28582(9)	0.28582(9)	0.28599(7)	0.28594(7)	0.28610(7)	0.28589(7)	0.28601(8)	0.28596(8)
O(11)	z	0.91855(18)	0.91856(18)	0.91839(13)	0.91839(14)	0.91847(14)	0.91828(15)	0.91848(15)	0.91863(15)
	U_{eq}	0.0063(2)	0.0063(2)	0.00602(17)	0.00614(19)	0.00617(19)	0.00618(19)	0.0059(2)	0.0061(2)
	x	0.27008(10)	0.26990(10)	0.26990(7)	0.26986(8)	0.26992(8)	0.26998(8)	0.26981(9)	0.27006(9)
O(12)	y	0.20974(10)	0.20955(10)	0.20948(7)	0.20952(8)	0.20950(8)	0.20964(8)	0.20944(8)	0.20969(9)
	z	0.55830(19)	0.55810(19)	0.55815(14)	0.55796(15)	0.55805(15)	0.55817(15)	0.55806(16)	0.55831(16)
	U_{eq}	0.0076(3)	0.0076(3)	0.00735(19)	0.0074(2)	0.0074(2)	0.0072(2)	0.0069(2)	0.0074(2)
H(4)	x	0.13312(14)	0.1384(14)	0.1325(11)	0.1320(11)	0.1294(11)	0.1316(12)	0.1293(12)	0.1350(12)
	y	0.8668(14)	0.8616(14)	0.8675(11)	0.8680(11)	0.8706(11)	0.8684(12)	0.8708(12)	0.8650(12)
	z	0.625(3)	0.625(3)	0.624(2)	0.622(2)	0.624(3)	0.623(3)	0.624(3)	0.626(3)
O(13)	U_{eq}	0.015	0.015	0.015	0.015	0.015	0.015	0.015	0.015

* The superscripts o and d on O(1) and O(2) denote the ordered and disordered atom coordinates for these sites.

** Fixed during the refinement.

TABLE 3 (cont'd). FINAL POSITIONS* AND EQUIVALENT ISOTROPIC-DISPLACEMENT PARAMETERS (\AA^2) OF ATOMS IN CRYSTALS OF LIDDICOATITE

		L22	L23	L24	L25	L26	L27	L28
X	x	0	0	0	0	0	0	0
	y	0	0	0	0	0	0	0
	z	0.7613(2)	0.76143(13)	0.76087(14)	0.76157(16)	0.76167(16)	0.76151(15)	0.76133(14)
Y	U_{eq}	0.0135(4)	0.0141(3)	0.0137(3)	0.0144(3)	0.0146(3)	0.0147(3)	0.0153(3)
	x	0.06180(7)	0.06195(4)	0.06187(5)	0.06196(5)	0.06181(5)	0.06183(5)	0.06210(4)
	y	0.93820(7)	0.93805(4)	0.93813(5)	0.93804(5)	0.93819(5)	0.93817(5)	0.93790(4)
Z	z	0.3644(3)	0.36442(16)	0.36431(18)	0.36551(18)	0.36473(19)	0.36530(18)	0.36663(16)
	U_{eq}	0.0093(6)	0.0104(4)	0.0110(4)	0.0098(4)	0.0117(4)	0.0112(4)	0.0104(3)
	x	0.25963(5)	0.25958(3)	0.25962(3)	0.25973(4)	0.25973(4)	0.25964(4)	0.25975(3)
T	y	0.29673(5)	0.29670(3)	0.29673(3)	0.29684(4)	0.29686(4)	0.29677(3)	0.29691(3)
	z	0.38811(13)	0.38819(8)	0.38823(9)	0.38806(10)	0.38801(10)	0.38811(9)	0.38799(8)
	U_{eq}	0.00570(16)	0.00602(9)	0.00610(10)	0.00601(11)	0.00606(11)	0.00613(10)	0.00619(10)
B	x	0.19025(4)	0.19019(3)	0.19019(3)	0.19018(3)	0.19014(3)	0.19022(3)	0.19019(3)
	y	0.19212(4)	0.19212(2)	0.19209(3)	0.19211(3)	0.19207(3)	0.19214(3)	0.19212(3)
	z	0	0	0	0	0	0	0
O(1) ^d	U_{eq}	0.00454(15)	0.00503(8)	0.00501(9)	0.00480(10)	0.00490(10)	0.00500(9)	0.00504(9)
	x	0.89128(13)	0.89117(8)	0.89119(9)	0.89103(10)	0.89129(10)	0.89123(10)	0.89101(9)
	y	0.10872(13)	0.10883(8)	0.10881(9)	0.10897(10)	0.10871(10)	0.10877(10)	0.10899(9)
O(1) ^o	z	0.5457(5)	0.5447(3)	0.5453(3)	0.5447(3)	0.5444(4)	0.5450(3)	0.5448(3)
	U_{eq}	0.0066(6)	0.0068(4)	0.0066(4)	0.0065(4)	0.0061(4)	0.0067(4)	0.0067(4)
	x	0.0109(2)	0.01083(13)	0.01087(14)	0.01128(14)	0.01074(15)	0.01099(14)	0.01123(13)
O(2) ^d	y	0.0217(4)	0.0217(3)	0.0217(3)	0.0226(3)	0.0215(3)	0.0220(3)	0.0225(3)
	z	0.2119(7)	0.2114(4)	0.2116(5)	0.2119(5)	0.2117(5)	0.2119(5)	0.2120(5)
	U_{eq}	0.0129(14)	0.0140(9)	0.0136(10)	0.0125(10)	0.0037(11)	0.0131(10)	0.0144(9)
O(2) ^o	x	0	0	0	0	0	0	0
	y	0	0	0	0	0	0	0
	z	0.2121(7)	0.2116(5)	0.2118(5)	0.2121(6)	0.2120(5)	0.2118(5)	0.2122(5)
O(3)	U_{eq}	0.0494(17)	0.0500(11)	0.0498(11)	0.0526(14)	0.0533(13)	0.0501(12)	0.0534(12)
	x	0.9317(3)	0.93117(19)	0.9310(2)	0.9308(2)	0.9312(2)	0.9307(2)	0.9309(2)
	y	0.0515(4)	0.05087(19)	0.0510(2)	0.0509(2)	0.0513(3)	0.0507(2)	0.0510(2)
O(4)	z	0.5196(4)	0.5195(2)	0.5192(2)	0.5194(3)	0.5192(3)	0.5198(3)	0.5198(2)
	U_{eq}	0.0103(7)	0.0088(4)	0.00864	0.0079(5)	0.0092(5)	0.0080(5)	0.0086(4)
	x	0.94016(9)	0.94020(6)	0.94008(6)	0.94003(8)	0.94003(7)	0.94003(7)	0.94000(7)
O(5)	y	0.05984(9)	0.05980(6)	0.05992(6)	0.05997(8)	0.05997(7)	0.05997(7)	0.06000(7)
	z	0.5198(4)	0.5197(3)	0.5195(3)	0.5196(3)	0.5199(3)	0.5198(3)	0.5199(3)
	U_{eq}	0.0167(6)	0.0162(4)	0.0160(4)	0.0157(5)	0.0160(4)	0.0159(4)	0.0160(4)
O(6)	x	0.13446(10)	0.13461(6)	0.13465(7)	0.13475(7)	0.13473(7)	0.13484(7)	0.13473(6)
	y	0.86554(10)	0.86539(6)	0.86535(7)	0.86525(7)	0.86527(7)	0.86516(7)	0.86527(6)
	z	0.4897(3)	0.4898(2)	0.4900(2)	0.4900(2)	0.4903(3)	0.4899(2)	0.4897(2)
O(7)	U_{eq}	0.0100(5)	0.0104(3)	0.0103(3)	0.0098(3)	0.0098(3)	0.0103(3)	0.0102(3)
	x	0.90789(9)	0.90778(6)	0.90786(6)	0.90785(7)	0.90784(7)	0.90794(6)	0.90788(6)
	y	0.09211(9)	0.09222(6)	0.09214(6)	0.09215(7)	0.09216(7)	0.09206(6)	0.09212(6)
O(8)	z	0.9251(3)	0.9251(2)	0.9252(2)	0.9255(2)	0.9254(2)	0.9255(2)	0.9257(2)
	U_{eq}	0.0075(4)	0.0082(3)	0.0080(3)	0.0081(3)	0.0083(3)	0.0084(3)	0.0084(3)
	x	0.09201(9)	0.09197(6)	0.09191(6)	0.09202(7)	0.09199(7)	0.09200(7)	0.09206(6)
O(9)	y	0.90799(9)	0.90803(6)	0.90809(6)	0.90798(7)	0.90801(7)	0.90800(7)	0.90794(6)
	z	0.9037(3)	0.90347(19)	0.9036(2)	0.9040(2)	0.9040(2)	0.9041(2)	0.9044(2)
	U_{eq}	0.0084(4)	0.0083(3)	0.0084(3)	0.0079(3)	0.0085(3)	0.0087(3)	0.0082(3)
O(10)	x	0.18584(12)	0.18598(7)	0.18601(8)	0.18627(9)	0.18617(9)	0.18609(8)	0.18633(7)
	y	0.19559(11)	0.19565(7)	0.19570(8)	0.19593(9)	0.19589(9)	0.19576(8)	0.19591(7)
	z	0.2238(3)	0.22363(15)	0.22385(16)	0.22362(18)	0.22343(18)	0.22360(17)	0.22364(15)
O(11)	U_{eq}	0.0066(3)	0.00692(19)	0.0074(2)	0.0068(2)	0.0071(2)	0.0068(2)	0.0071(2)
	x	0.28535(11)	0.28533(7)	0.28541(7)	0.28533(8)	0.28545(8)	0.28528(8)	0.28542(7)
	y	0.28610(11)	0.28597(7)	0.28595(8)	0.28590(8)	0.28601(8)	0.28590(8)	0.28587(7)
O(12)	z	0.9183(2)	0.91836(14)	0.91837(15)	0.91835(17)	0.91837(17)	0.91825(16)	0.91841(14)
	U_{eq}	0.0061(3)	0.00607(18)	0.0062(2)	0.0062(2)	0.0061(2)	0.0063(2)	0.00608(19)
	x	0.26992(12)	0.26995(7)	0.26994(8)	0.27008(9)	0.26993(9)	0.26999(9)	0.26994(8)
O(13)	y	0.20946(12)	0.20957(7)	0.20947(8)	0.20966(9)	0.20961(9)	0.20960(8)	0.20957(8)
	z	0.5582(2)	0.55790(14)	0.55795(16)	0.55791(18)	0.55783(17)	0.55798(16)	0.55782(15)
	U_{eq}	0.0072(3)	0.00736(19)	0.0074(2)	0.0075(2)	0.0073(2)	0.0073(2)	0.0076(2)
H(3)	x	0.1307(18)	0.1308(11)	0.1328(12)	0.1316(14)	0.1272(13)	0.1312(12)	0.1339(11)
	y	0.8693(18)	0.8692(11)	0.8672(12)	0.8684(14)	0.8728(13)	0.8688(12)	0.8661(11)
	z	0.625(3)	0.622(2)	0.623(2)	0.623(3)	0.618(3)	0.622(3)	0.625(2)
U _{eq}	**	0.015	0.015	0.015	0.015	0.015	0.015	0.015

* The superscripts o and d on O(1) and O(2) denote the ordered and disordered atom coordinates for these sites.

** Fixed during the refinement.

TABLE 4. INTERATOMIC DISTANCES (Å) IN LIDDICOATITE

	L1	L2	L4	L5	L6	L7	L11	L12
X–O(2) ^a ×3	2.389(2)	2.381(2)	2.386(2)	2.381(2)	2.381(2)	2.379(2)	2.386(2)	2.384(2)
X–O(4) ^a ×3	2.797(2)	2.795(2)	2.795(2)	2.790(2)	2.789(2)	2.786(2)	2.803(2)	2.799(2)
X–O(5) ^a ×3	2.737(2)	2.730(2)	2.733(2)	2.729(2)	2.726(2)	2.723(2)	2.742(2)	2.736(2)
<X–O>	2.641	2.635	2.638	2.633	2.632	2.629	2.644	2.640
Y–O(1) ^d	1.781(4)	1.776(4)	1.776(4)	1.771(4)	1.770(4)	1.771(4)	1.778(4)	1.782(4)
Y–O(1) ^d ×2	2.189(3)	2.183(3)	2.178(3)	2.174(3)	2.170(3)	2.165(3)	2.206(3)	2.192(3)
Y–O(2) ^d ×2	1.885(3)	1.884(3)	1.889(3)	1.892(3)	1.893(3)	1.895(3)	1.882(3)	1.881(3)
Y–O(2) ^d ×2	2.107(3)	2.107(3)	2.101(3)	2.109(3)	2.109(3)	2.106(3)	2.111(3)	2.108(3)
Y–O(3)	2.179(2)	2.180(2)	2.179(2)	2.182(2)	2.189(2)	2.187(2)	2.179(2)	2.179(2)
Y–O(6) ^a ×2	2.009(1)	2.001(1)	2.000(2)	1.995(2)	1.990(2)	1.987(1)	2.016(1)	2.010(2)
Y–O(1) ^e	2.037(3)	2.031(2)	2.029(3)	2.024(3)	2.022(2)	2.019(2)	2.045(4)	2.039(3)
Y–O(2) ^e ×2	1.994(2)	1.993(2)	1.993(2)	1.998(2)	2.000(2)	1.999(2)	1.994(2)	1.992(2)
Y–O(3)	2.178(2)	2.180(2)	2.178(3)	2.182(2)	2.189(2)	2.186(2)	2.178(2)	2.178(3)
Y–O(6) ^e ×2	2.008(2)	2.001(2)	2.000(2)	1.994(2)	1.990(2)	1.987(2)	2.016(2)	2.010(2)
<Y–O>	2.037	2.033	2.032	2.032	2.032	2.030	2.041	2.037
Z–O(3)	1.949(1)	1.944(1)	1.947(1)	1.943(1)	1.942(1)	1.941(1)	1.950(1)	1.947(1)
Z–O(6)	1.848(1)	1.847(1)	1.849(1)	1.849(1)	1.847(1)	1.848(1)	1.846(1)	1.846(1)
Z–O(7)	1.883(1)	1.884(1)	1.885(1)	1.886(1)	1.887(1)	1.885(1)	1.883(1)	1.885(1)
Z–O(7)	1.960(1)	1.961(1)	1.958(1)	1.961(1)	1.961(1)	1.960(1)	1.960(1)	1.960(1)
Z–O(8)	1.886(1)	1.887(1)	1.887(1)	1.887(1)	1.887(1)	1.888(1)	1.885(1)	1.886(1)
Z–O(8)	1.906(1)	1.906(1)	1.905(1)	1.902(1)	1.902(1)	1.903(1)	1.906(1)	1.906(1)
<Z–O>	1.905	1.905	1.905	1.905	1.904	1.904	1.905	1.905
T–O(4)	1.626(1)	1.627(1)	1.626(1)	1.628(1)	1.627(1)	1.626(1)	1.627(1)	1.626(1)
T–O(5)	1.642(1)	1.642(1)	1.642(1)	1.644(1)	1.643(1)	1.642(1)	1.642(1)	1.642(1)
T–O(6)	1.594(1)	1.593(1)	1.593(1)	1.592(1)	1.592(1)	1.592(1)	1.594(1)	1.595(2)
T–O(7)	1.607(1)	1.607(1)	1.608(1)	1.605(1)	1.605(1)	1.606(1)	1.607(1)	1.607(1)
<T–O>	1.617	1.617	1.617	1.617	1.617	1.617	1.618	1.618
B–O(2)	1.362(3)	1.367(3)	1.359(3)	1.360(3)	1.360(3)	1.358(3)	1.363(3)	1.360(3)
B–O(8) ^a ×2	1.384(2)	1.382(2)	1.385(2)	1.386(2)	1.385(2)	1.384(2)	1.383(2)	1.385(2)
<B–O>	1.377	1.377	1.376	1.377	1.377	1.375	1.376	1.377

Figure 3 suggest a $[^{14}\text{B}]$ content of ~0.01–0.02 apfu. The remaining spectra indicate that neither $[^{14}\text{Al}]$ nor $[^{14}\text{B}]$ is present in quantities detectable by MAS NMR in this crystal.

Ultrahigh-field NMR (21.1 T) and ultrafast MAS (62 kHz) were used in conjunction on one sample to reduce the second-order quadrupolar broadening and minimize any paramagnetic interactions. The $[^{16}\text{Al}]$ peak narrowed by a factor of 2 in ppm relative to the 14.1 T data, thereby increasing the spectral resolution and verifying that no $[^{14}\text{Al}]$ signal is evident (data not shown).

A requirement for MAS NMR spectroscopy is that the sample under investigation be low in paramagnetic constituents (*e.g.*, Fe^{2+} , Mn^{2+}). In a detailed study of $[^{11}\text{B}]$ and $[^{27}\text{Al}]$ MAS NMR spectra collected on 50 different samples of tourmaline, Lussier *et al.* (2009) showed that in samples with extremely low contents of paramagnetic ions ($\text{Fe}^{2+} + \text{Mn}^{2+} < 0.05 \text{ apfu}$), $[^{14}\text{B}]$ and $[^{14}\text{Al}]$ signals are easily resolved by MAS NMR, but the presence of greater than ~0.1 apfu transition metals may degrade the spectrum considerably through signal broadening, thereby increasing the limit of detection of tetrahedrally coordinated species.

Limits of detectability of $[^{14}\text{B}]$ and $[^{14}\text{Al}]$ in liddicoatite by MAS NMR

We decided to investigate the limit of detectability of [4]-coordinated B and Al in tourmaline by $[^{11}\text{B}]$ and $[^{27}\text{Al}]$ MAS NMR by simulation. We took the experimental spectra shown in Figures 2a,d and 3a,d (in order to accommodate the peak broadening expected for samples containing different amounts of paramagnetic constituents) and added component peaks at 0 and 70 ppm corresponding to [4]-coordinated B and Al in tourmaline (Lussier *et al.* 2008a, 2009), with relative intensities corresponding to a range of amounts of [4]-coordinated B and Al from 0.15 to 0.005 apfu. The widths of the inserted peaks were calculated in the following manner. The ratios of the widths of the $[^{13}\text{B}]$ and $[^{14}\text{B}]$ peaks and the $[^{14}\text{Al}]$ and $[^{16}\text{Al}]$ peaks in the spectra of Lussier *et al.* (2009) were used to calculate the widths of the $[^{14}\text{B}]$ and $[^{14}\text{Al}]$ peaks in the simulated spectra. The results are shown in Figure 4; peaks corresponding to [4]-coordinated B and Al are discernable down to $[^{14}\text{B}]$ and $[^{14}\text{Al}]$ contents of 0.02 and 0.01 apfu for low contents of paramagnetic ions (<0.04 apfu) and

TABLE 4 (cont'd). INTERATOMIC DISTANCES (Å) IN LIDDICOATITE

	L13	L15	L16	L17	L18	L19	L20	L21
X–O(2) ×3	2.397(2)	2.386(2)	2.379(2)	2.388(2)	2.382(2)	2.385(2)	2.382(2)	2.391(2)
X–O(4) ×3	2.787(2)	2.780(2)	2.781(2)	2.782(2)	2.780(2)	2.779(2)	2.779(2)	2.783(2)
X–O(5) ×3	2.724(2)	2.716(2)	2.718(2)	2.718(2)	2.717(2)	2.720(2)	2.715(2)	2.719(2)
<X–O>	2.636	2.627	2.626	2.629	2.626	2.628	2.625	2.631
Y–O(1) ^d	1.768(5)	1.765(5)	1.770(3)	1.764(4)	1.772(4)	1.767(4)	1.768(4)	1.767(4)
Y–O(1) ^d ×2	2.165(4)	2.153(4)	2.156(3)	2.158(3)	2.153(3)	2.157(3)	2.151(3)	2.159(3)
Y–O(2) ^d ×2	1.895(3)	1.894(3)	1.899(3)	1.897(3)	1.901(3)	1.900(3)	1.898(3)	1.895(3)
Y–O(2) ^d ×2	2.108(3)	2.112(3)	2.105(2)	2.103(3)	2.105(3)	2.107(3)	2.103(3)	2.109(3)
Y–O(3)	2.179(3)	2.189(3)	2.186(2)	2.185(2)	2.185(2)	2.185(2)	2.192(2)	2.184(2)
Y–O(6) ×2	1.990(2)	1.976(2)	1.979(1)	1.982(1)	1.977(1)	1.978(1)	1.979(2)	1.984(1)
Y–O(1) ^o	2.018(3)	2.010(3)	2.013(2)	2.012(2)	2.012(2)	2.013(2)	2.009(2)	2.013(3)
Y–O(2) ^o ×2	1.999(2)	2.000(2)	2.000(1)	1.998(2)	2.001(2)	2.001(2)	1.999(2)	1.999(2)
Y–O(3)	2.179(3)	2.187(3)	2.185(2)	2.185(2)	2.184(2)	2.184(2)	2.191(3)	2.179(3)
Y–O(6) ×2	1.989(2)	1.975(2)	1.978(1)	1.981(2)	1.977(2)	1.978(2)	1.978(2)	1.983(2)
<Y–O>	2.029	2.025	2.026	2.026	2.025	2.026	2.026	2.026
Z–O(3)	1.944(1)	1.939(1)	1.940(1)	1.941(1)	1.941(1)	1.941(1)	1.941(1)	1.943(1)
Z–O(6)	1.849(1)	1.853(2)	1.850(1)	1.849(1)	1.848(1)	1.851(1)	1.850(1)	1.849(1)
Z–O(7)	1.886(1)	1.887(1)	1.886(1)	1.885(1)	1.886(1)	1.887(1)	1.885(1)	1.887(1)
Z–O(7)	1.962(1)	1.963(1)	1.961(1)	1.961(1)	1.960(1)	1.963(1)	1.960(1)	1.961(1)
Z–O(8)	1.884(1)	1.888(1)	1.888(1)	1.889(1)	1.888(1)	1.887(1)	1.890(1)	1.885(1)
Z–O(8)	1.904(1)	1.899(1)	1.901(1)	1.901(1)	1.901(1)	1.901(1)	1.900(1)	1.902(1)
<Z–O>	1.905	1.905	1.904	1.904	1.904	1.905	1.904	1.905
T–O(4)	1.628(1)	1.627(1)	1.627(1)	1.627(1)	1.627(1)	1.628(1)	1.627(1)	1.627(1)
T–O(5)	1.643(1)	1.642(1)	1.643(1)	1.643(1)	1.643(1)	1.643(1)	1.644(1)	1.643(1)
T–O(6)	1.594(1)	1.589(2)	1.591(1)	1.592(1)	1.592(1)	1.591(1)	1.591(1)	1.593(1)
T–O(7)	1.604(1)	1.602(1)	1.605(1)	1.605(1)	1.606(1)	1.604(1)	1.606(1)	1.604(1)
<T–O>	1.617	1.615	1.617	1.617	1.617	1.617	1.617	1.617
B–O(2)	1.363(4)	1.361(4)	1.360(3)	1.359(3)	1.359(3)	1.363(3)	1.359(3)	1.361(3)
B–O(8) ×2	1.383(2)	1.383(2)	1.385(1)	1.385(2)	1.385(2)	1.385(2)	1.385(2)	1.386(2)
<B–O>	1.376	1.376	1.377	1.376	1.376	1.378	1.376	1.378

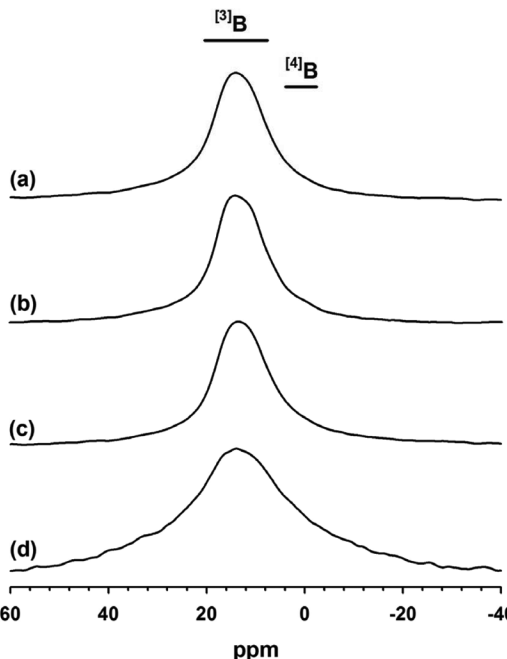


FIG. 2. ^{11}B MAS NMR spectra of liddicoatite: (a) NMR 1; (b) NMR 2; (c) NMR 3; (d) NMR 4.

TABLE 4 (cont'd). INTERATOMIC DISTANCES (Å) IN LIDDICOATITE

	L22	L23	L24	L25	L26	L27	L28
X-O(2) ^a ×3	2.379(3)	2.380(2)	2.381(2)	2.387(2)	2.387(2)	2.383(2)	2.383(2)
X-O(4) ^a ×3	2.780(3)	2.783(2)	2.783(2)	2.784(2)	2.783(2)	2.780(2)	2.784(2)
X-O(5) ^a ×3	2.718(3)	2.716(2)	2.716(2)	2.720(2)	2.718(2)	2.719(2)	2.722(2)
<X-O>	2.626	2.626	2.627	2.630	2.629	2.627	2.630
Y-O(1) ^d	1.767(6)	1.773(4)	1.769(4)	1.768(4)	1.773(4)	1.770(4)	1.776(4)
Y-O(1) ^d ×2	2.154(4)	2.158(3)	2.156(3)	2.169(3)	2.155(3)	2.160(3)	2.175(3)
Y-O(2) ^d ×2	1.904(5)	1.899(3)	1.898(3)	1.895(3)	1.900(2)	1.894(3)	1.895(3)
Y-O(2) ^d ×2	2.100(4)	2.108(2)	2.107(3)	2.110(3)	2.103(3)	2.110(3)	2.106(3)
Y-O(3)	2.182(3)	2.182(2)	2.186(2)	2.184(2)	2.190(2)	2.189(2)	2.176(2)
Y-O(6) ^d ×2	1.978(2)	1.979(1)	1.979(1)	1.987(2)	1.985(2)	1.985(2)	1.990(1)
Y-O(1) ^o	2.011(3)	2.016(2)	2.013(2)	2.020(3)	2.013(3)	2.016(2)	2.027(2)
Y-O(2) ^o ×2	2.000(2)	2.001(1)	2.001(2)	2.000(2)	1.999(2)	2.000(2)	1.999(1)
Y-O(3)	2.181(3)	2.181(2)	2.185(2)	2.183(3)	2.187(3)	2.188(3)	2.175(2)
Y-O(6) ^o ×2	1.977(2)	1.978(1)	1.979(2)	1.987(2)	1.985(2)	1.985(2)	1.989(2)
<Y-O ^o >	2.024	2.026	2.026	2.030	2.028	2.029	2.030
Z-O(3)	1.941(1)	1.940(1)	1.940(1)	1.943(1)	1.943(1)	1.940(1)	1.942(1)
Z-O(6)	1.849(2)	1.849(1)	1.848(1)	1.848(1)	1.849(1)	1.848(1)	1.848(1)
Z-O(7)	1.886(2)	1.886(1)	1.885(1)	1.886(1)	1.885(1)	1.886(1)	1.885(1)
Z-O(7)	1.959(2)	1.962(1)	1.961(1)	1.962(1)	1.959(1)	1.962(1)	1.961(1)
Z-O(8)	1.888(2)	1.888(1)	1.889(1)	1.887(1)	1.887(1)	1.887(1)	1.887(1)
Z-O(8)	1.902(2)	1.900(1)	1.901(1)	1.902(1)	1.901(1)	1.901(1)	1.902(1)
<Z-O>	1.904	1.904	1.904	1.905	1.904	1.904	1.904
T-O(4)	1.627(1)	1.627(1)	1.627(1)	1.628(1)	1.627(1)	1.627(1)	1.627(1)
T-O(5)	1.644(1)	1.644(1)	1.644(1)	1.644(1)	1.643(1)	1.643(1)	1.642(1)
T-O(6)	1.593(2)	1.592(1)	1.593(1)	1.592(1)	1.590(1)	1.592(1)	1.592(1)
T-O(7)	1.605(2)	1.604(1)	1.605(1)	1.605(1)	1.607(1)	1.604(1)	1.605(1)
<T-O>	1.617	1.617	1.617	1.617	1.617	1.617	1.617
B-O(2)	1.358(4)	1.362(3)	1.359(3)	1.363(3)	1.354(3)	1.357(3)	1.362(3)
B-O(8) ^b ×2	1.384(2)	1.385(2)	1.383(2)	1.385(2)	1.388(2)	1.386(2)	1.383(2)
<B-O>	1.375	1.377	1.375	1.378	1.377	1.376	1.376

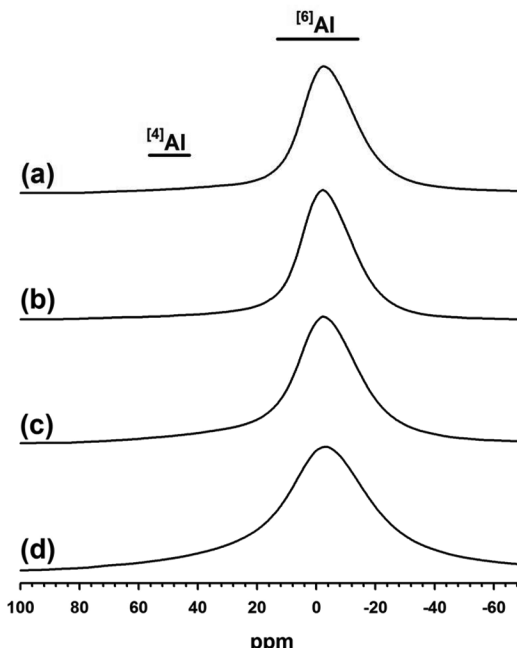


FIG. 3. ^{27}Al MAS NMR spectra of liddicoatite: (a) NMR 1; (b) NMR 2; (c) NMR 3; (d) NMR 4.

0.08 and 0.01 *apfu* for slightly higher contents (~0.12 *apfu*). From this exercise, we may conclude that $^{[4]}B$ is less than 0.02 and $^{[4]}Al$ is less than 0.01 *apfu* in all the samples examined here.

^{57}Fe Mössbauer spectroscopy

The Mössbauer spectra are shown in Figure 5. As expected, the majority of the Fe in both sectors is divalent, but a small amount of Fe^{3+} is present in each sector: 9% and 5% in the pyramid and prism sectors, respectively. There are two doublets assigned to Fe^{2+} in octahedral coordination (Table 7), and their Mössbauer hyperfine parameters (Hawthorne 1988) are in accord with the doublets Y1 and Y2 of Andreozzi *et al.* (2008), which are assigned to Fe^{2+} at Y with different next-nearest-neighbor arrangements.

SITE POPULATIONS

Site populations were assigned on the basis of (1) refined site-scattering values (Table 5), (2) the unit formulae calculated from the electron-microprobe analyses (Table 6), (3) the results of MAS NMR spectroscopy (Figs. 2 and 3), and (4) mean bond-lengths (Table 4).

Refinement of T-site scattering in tourmaline

We refined the T-site scattering by considering the T site as occupied by Si and B, with the sum of their occupancies constrained to unity. A key issue in such a procedure is the type of scattering factors used for the refinement. In least-squares refinement of a crystal structure, the magnitudes of the calculated structure-factors are scaled to the magnitudes of the observed structure-factors by the scale factor, and there is a relatively strong correlation between the scale factor and the refined site-scattering factors. If all site-scattering factors in a crystal structure are considered as variable, the shift matrix becomes singular, and the refinement fails. It is necessary that the scattering for some of the atoms in the structure be fixed such that the refined site-scattering values are correctly scaled, and the atoms thus fixed should constitute a significant fraction of the total scattering (preferably significantly greater than 50%) in order that the scaling be reasonably accurate. This scaling is affected by the type of scattering factors used for the atoms, *i.e.*, ionized or neutral. The total scattering for an ionized species is less than that for a neutral species for cations, and the inverse for anions. Hence the type of scattering factors used will affect the total refined site-scattering both directly through the scattering factors of the refined species (usually cations), and indirectly through the scattering factors of the nonrefined species (commonly anions). This issue was investigated in detail for the structure of korner-

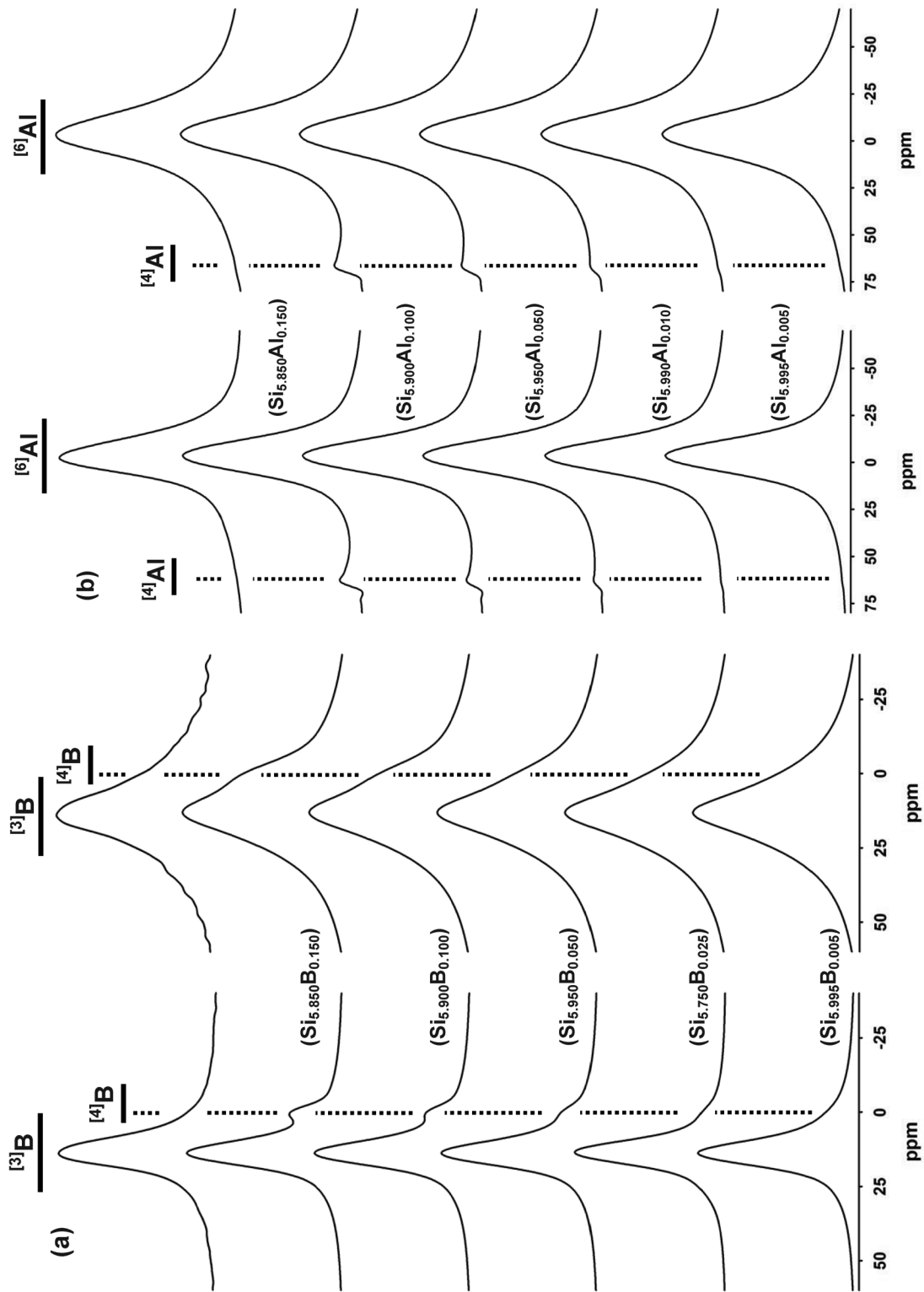
pine, $XM_9T_5O_{21}(OH,F)$ where $X = \square$, Fe^{2+} , Mg ; $M = Al$, Mg , Fe^{2+} , Fe^{3+} ; $T = Si$, Al , B (Cooper *et al.* 2009), in which the three tetrahedrally coordinated T sites are occupied by Si, Al and B. The scattering at the M sites is ~1 *epfu* larger using an ionized scattering factor rather than a neutral scattering factor for oxygen (Fig. 6a). The site scattering at the partly occupied X site is in accord with that determined by EMPA and SIMS for refinement with an ionized scattering factor for oxygen (Fig. 6b), whereas the values determined using a neutral scattering factor for oxygen deviate from the values determined by EMPA–SIMS by ~1.1 *epfu*. These results suggest that the refined values of B at the T site in tourmaline should be sensitive to the type of scattering factors used. Here, we have investigated the effects of the use of different scattering curves on the refinement of site-scattering values in tourmaline, focusing on the occurrence of B at the T site.

We refined all structures of liddicoatite in four different ways under the constraint that $Si + ^{[4]}B = 6$ *apfu*, and obtained different values for the T-site occupancy of $^{[4]}B$ for each different set of scattering factors used. The results are summarized in Figure 7. Refinement with ionized scattering-curves for O and Si failed because refinement converged toward negative occupancy values for $^{[4]}B$. In this case, we set the occupancy of the T site to Si only and refined the occupancy, getting values less than 1. We then recalculated the cations as

TABLE 5. SITE-SCATTERING VALUES (*epfu*) FOR LIDDICOATITE FROM MADAGASCAR, DERIVED FROM SREF AND EMPA

	X site		Y site	
	SREF	EMPA	SREF	EMPA
L1	16.9(1)	16.3	31.7(2)	32.0
L2	17.9(1)	17.3	28.7(2)	28.6
L4	17.2(1)	16.3	29.1(2)	29.0
L5	18.2(1)	17.7	26.5(2)	25.9
L6	18.3(1)	17.9	26.3(2)	25.4
L7	18.1(1)	17.5	25.6(2)	25.3
L11	16.9(1)	16.1	32.5(2)	32.9
L12	17.6(1)	16.8	30.5(2)	30.9
L13	16.3(1)	16.0	27.4(2)	27.1
L15	17.6(1)	17.2	23.8(3)	23.0
L16	17.6(1)	17.2	23.8(2)	24.1
L17	17.1(1)	16.7	25.0(2)	25.3
L18	17.5(1)	17.1	23.3(2)	23.9
L19	17.4(1)	17.1	23.8(2)	23.7
L20	17.4(1)	16.9	23.6(2)	23.9
L21	16.9(1)	16.4	25.5(2)	25.5
L22	17.3(1)	16.9	23.7(3)	24.0
L23	17.4(1)	17.1	23.8(2)	24.5
L24	17.8(1)	17.4	23.8(2)	23.9
L25	16.9(1)	16.3	25.4(2)	25.2
L26	17.1(1)	16.8	25.7(2)	26.9
L27	17.4(1)	16.2	25.2(2)	27.1
L28	17.2(1)	16.4	25.9(2)	23.9
<dev.> *	0.6		0.5	

* <dev.>: mean deviation.



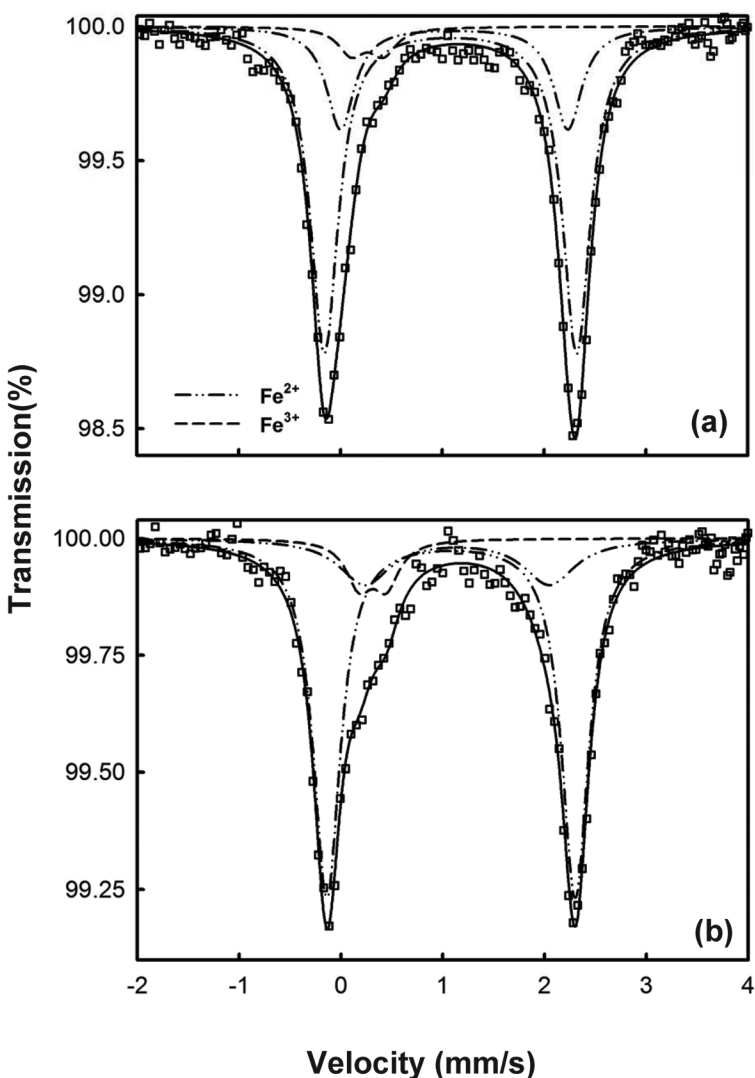


FIG. 5. Mössbauer spectra for liddicoatite: (a) prism sector; (b) pyramid sector.

FIG. 4. ^{11}B and ^{27}Al MAS NMR spectra of liddicoatite samples NMR1 [left, in both (a) and (b)] and NMR4 [right, in both (a) and (b)] with additional simulated peaks added at the positions for (a) ^{14}B (~ 0 ppm) and (b) ^{14}Al (~ 70 ppm) for various contents of ^{14}B and ^{14}Al in *apfu* (indicated on the figure).

Si and B under the constraint that $\text{Si} + \text{B} = 1$, arriving at small negative occupancy values for ^{14}B . The grand mean ^{14}B content of the *T* site varies from -0.04 apfu for ionized scattering-curves for O and Si to 0.25 apfu for neutral scattering-curves for O and Si. No ^{14}B was detected in the liddicoatite samples examined here by ^{11}B MAS NMR, and the simulation results of Figure 4 suggests limits of detection of the order of 0.02 apfu . This result is in accord with our refinement results using ionized scattering-curves for O and Si, suggesting that use of these curves is giving more accurate results for *T*-site populations than refinement with neutral

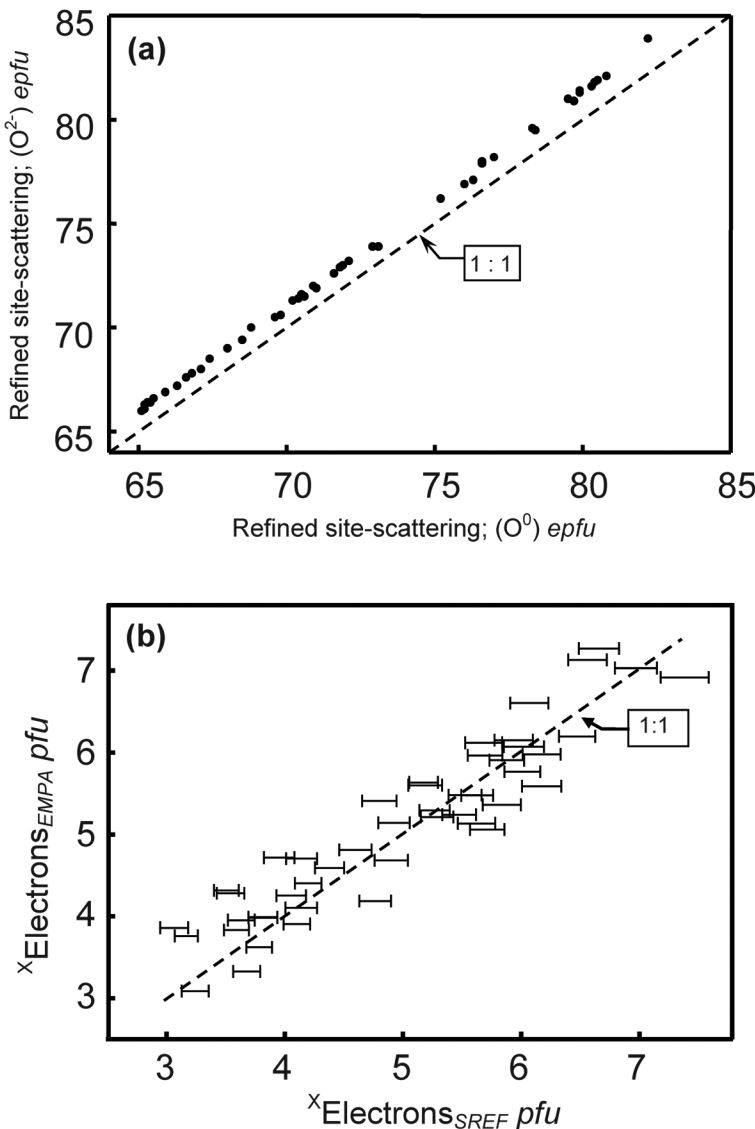


FIG. 6. Results for kornerupine; (a) comparison of the site-scattering at the $[X + M(1,2,4)]$ sites refined using ionized (O^{2-}) and neutral (O^0) X-ray scattering factors; (b) comparison of the X -site scattering derived by crystal-structure refinement (SREF) using an ionized scattering-factor for oxygen and the effective scattering calculated from the unit formula derived from the electron-microprobe analysis; the dashed line indicates the 1 : 1 relation, and the lines through the data points represent ± 1 standard deviation in this and the following figures. Modified from Cooper *et al.* (2009).

scattering factors. Moreover, our refinements using neutral scattering factors for O and Si gave ${}^{[4]}B$ T-site populations of ~ 0.25 apfu, values that should easily be observed by ${}^{11}B$ MAS NMR (see above).

The T site

In all MAS NMR spectra, there is no evidence of $[4]$ -coordinated B or Al in this crystal (Figs. 2, 3). These results are in accord with the observed $\langle T-O \rangle$ bond

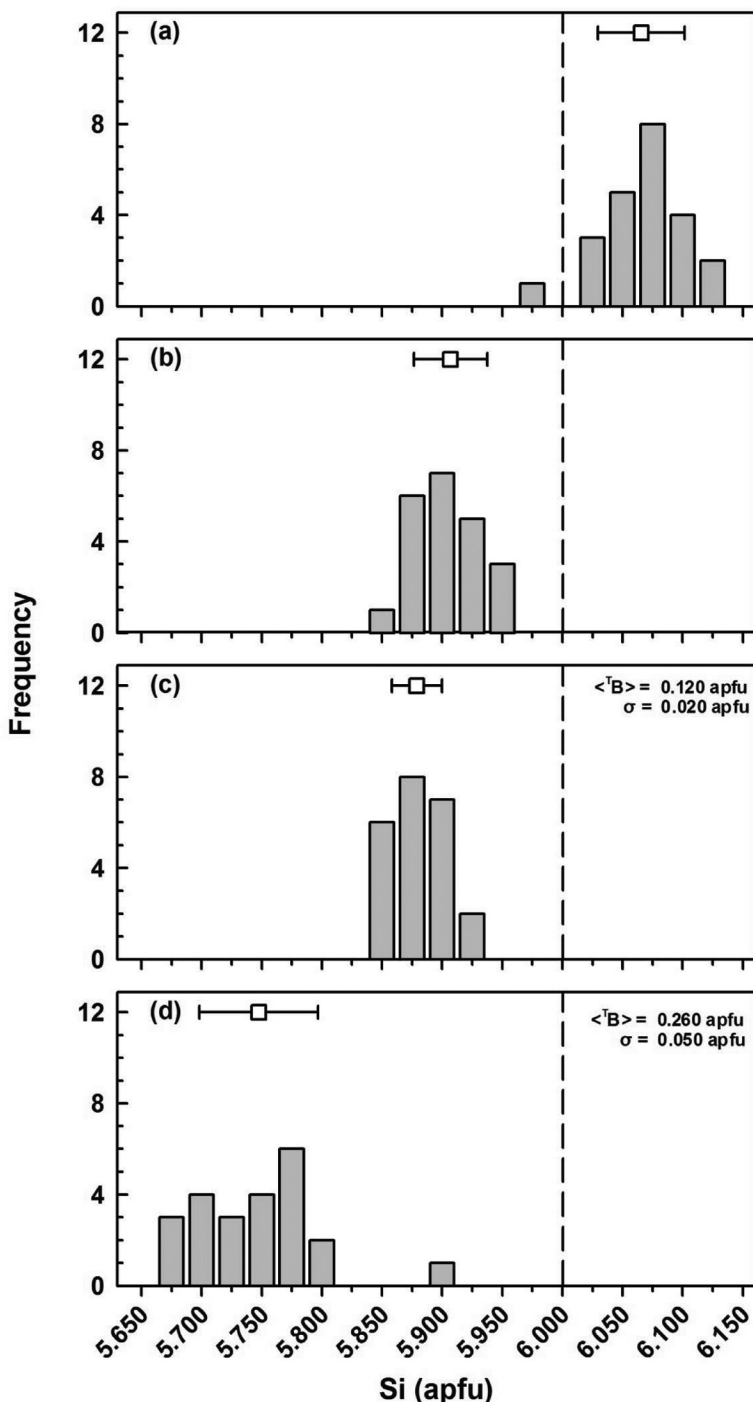


FIG. 7. Variation in refined site-population for the T site in the liddicoatite fragments of this work using the following scattering factors: (a) Si^{4+} and O^{2-} ; (b) Si^{4+} and O^0 ; (c) Si^0 and O^{2-} ; (d) Si^0 and O^0 .

TABLE 6. CHEMICAL COMPOSITIONS AND UNIT FORMULAE OF LIDDICOATITE

	L1	L2	L4	L5	L6	L7	L11	L12	L13	L15	L16
SiO ₂ wt.%	36.81	37.01	37.30	37.25	37.28	37.63	36.88	36.59	37.69	37.98	37.43
TiO ₂	0.03	0.01	0.02	0.01	0.01	0.02	0.00	0.01	0.08	0.01	0.02
Al ₂ O ₃	38.35	38.08	38.24	38.19	38.25	38.82	37.83	37.70	38.87	39.35	39.08
B ₂ O ₃	10.85	10.84	10.92	10.88	10.89	11.01	10.81	10.74	11.05	11.11	10.99
Fe ₂ O ₃	0.07	0.01	0.06	0.01	0.01	0.03	0.02	0.02	0.13	0.02	0.04
FeO	0.76	0.11	0.63	0.15	0.14	0.32	0.18	0.18	1.38	0.21	0.42
MgO	0.00	0.00	0.43	0.00	0.00	0.01	0.00	0.00	0.26	0.00	0.00
MnO	2.67	2.42	1.74	1.54	1.34	1.00	3.89	3.09	0.25	0.24	0.26
CaO	2.84	3.28	3.03	3.67	3.75	3.76	2.56	2.94	3.46	4.15	4.04
PbO	0.50	0.60	0.48	0.53	0.53	0.46	0.58	0.59	0.14	0.23	0.24
Na ₂ O	1.40	1.14	1.25	0.96	0.93	0.92	1.51	1.30	1.13	0.75	0.80
Li ₂ O	2.00	2.26	2.18	2.47	2.50	2.51	1.98	2.09	2.36	2.67	2.54
H ₂ O	3.08	3.09	3.21	3.10	3.10	3.12	3.10	3.01	3.19	3.19	3.14
F	1.40	1.37	1.17	1.39	1.38	1.42	1.34	1.47	1.30	1.35	1.37
O=F	-0.59	-0.58	-0.49	-0.59	-0.58	-0.60	-0.56	-0.62	-0.55	-0.57	-0.58
Σ	100.17	99.64	100.17	99.56	99.53	100.43	100.12	99.11	100.74	100.69	99.79
Si ⁴⁺ apfu	5.895	5.933	5.937	5.948	5.948	5.942	5.927	5.921	5.931	5.944	5.921
B ³⁺	3.000	3.000	3.000	3.000	3.000	3.000	3.000	3.000	3.000	3.000	3.000
Al ³⁺	6.000	6.000	6.000	6.000	6.000	6.000	6.000	6.000	6.000	6.000	6.000
Ti ⁴⁺	0.004	0.001	0.002	0.001	0.001	0.002	0.000	0.001	0.009	0.001	0.002
Al ³⁺	1.238	1.194	1.174	1.187	1.193	1.224	1.166	1.190	1.209	1.258	1.286
Fe ³⁺	0.009	0.001	0.007	0.002	0.002	0.004	0.002	0.002	0.016	0.002	0.005
Fe ²⁺	0.101	0.015	0.084	0.019	0.018	0.042	0.025	0.025	0.181	0.027	0.055
Mg ²⁺	0.000	0.000	0.102	0.000	0.000	0.002	0.000	0.000	0.061	0.000	0.000
Mn ²⁺	0.362	0.329	0.235	0.208	0.181	0.134	0.530	0.424	0.033	0.032	0.035
Li ⁺	1.286	1.460	1.396	1.583	1.605	1.592	1.277	1.358	1.491	1.680	1.617
ΣY	3.000	3.000	3.000	3.000	3.000	3.000	3.000	3.000	3.000	3.000	3.000
Ca ²⁺	0.487	0.563	0.517	0.628	0.641	0.636	0.441	0.510	0.583	0.696	0.685
Na ⁺	0.435	0.354	0.386	0.297	0.288	0.282	0.471	0.408	0.345	0.228	0.245
Pb ²⁺	0.022	0.026	0.021	0.023	0.023	0.020	0.025	0.026	0.006	0.010	0.010
□	0.056	0.057	0.076	0.052	0.048	0.062	0.063	0.056	0.066	0.066	0.060
ΣX	1.000	1.000	1.000	1.000	1.000	1.000	1.000	1.000	1.000	1.000	1.000
OH ⁻	3.291	3.306	3.411	3.298	3.304	3.291	3.319	3.248	3.353	3.332	3.315
F ⁻	0.709	0.694	0.589	0.702	0.696	0.709	0.681	0.752	0.647	0.668	0.685
$\Sigma(V+W)$	4.000	4.000	4.000	4.000	4.000	4.000	4.000	4.000	4.000	4.000	4.000

lengths (Table 4), which range from 1.616 to 1.619 Å (avg. = 1.6174 Å, $<\text{st.dev.}>$ = 0.0007 Å). Hence, we conclude that for this crystal, there are 6 Si *apfu* at the *T* site. Formula normalization of the results of all the chemical analyses done on this crystal yields a range of values $5.90 < \text{Si} < 5.97 \text{ apfu}$ with a mean value of $5.93 \pm 0.02 \text{ apfu}$. Above, we concluded from the ¹¹B and ²⁷Al MAS NMR spectra that ^{[4]B} is less than 0.02 *apfu* and ^{[4]Al} is less than 0.01 *apfu* in this crystal of liddicoatite, indicating the Si should be greater than 5.97 *apfu* in these crystals. The difference between the mean observed Si content of 5.93(2) *apfu* and the value of 5.97 *apfu* is 0.04(2) *apfu*, a value that is not significantly different from zero at the 99% confidence limit. If we assume a Si value of 6.00 *apfu* in these crystals, the difference between the average observed value and our assumed value is 0.07(2) *apfu*, a value that is marginally significant at the 99% confidence limit. Incorporation

of small amounts of ^{[4]B} or ^{[4]Al} at the *T* sites would change the $\langle T\text{-O} \rangle$ distances by less than 0.002 Å, of the same order of magnitude as the standard deviations on the distances, and hence provide no evidence of deviation from 6.00 Si *apfu*. The observed $\langle T\text{-O} \rangle$ distances are in the range 1.616–1.619 Å, close to the ideal $\langle ^7\text{Si-O} \rangle$ distance (in the tourmaline structure), 1.620 Å, given by MacDonald & Hawthorne (1995).. Thus we presume that there is a small but systematic error (that we have been unable to find) in our electron-microprobe data and assign our *T*-site occupancies as 6.00 Si *apfu*.

Ertl *et al.* (2006) reported structure and chemical data on four fragments of a crystal of liddicoatite from Anjanabonoina, Madagascar. They analyzed the crystals for B by SIMS and reported 0.14–0.57 *apfu* ^{[4]B}. This amount of ^{[4]B} would easily be detected by ¹¹B MAS NMR, and hence we must conclude that the two samples of liddicoatite differ significantly in their *T*-site contents.

TABLE 6 (cont'd). CHEMICAL COMPOSITIONS AND UNIT FORMULAE OF LIDDICOATITE

	L17	L18	L19	L20	L21	L22	L23	L24	L25	L26	L27	L28
SiO ₂ wt.%	37.45	37.35	37.50	37.77	37.62	37.71	37.12	37.64	38.16	37.33	37.19	37.36
TiO ₂	0.04	0.02	0.02	0.02	0.06	0.03	0.03	0.01	0.06	0.08	0.14	0.10
Al ₂ O ₃	39.21	39.36	39.20	39.58	39.04	38.99	39.06	39.33	38.71	38.25	38.86	38.57
B ₂ O ₃	11.01	10.99	11.00	11.10	11.03	11.04	10.94	11.05	11.10	10.89	10.95	10.97
Fe ₂ O ₃	0.07	0.02	0.03	0.04	0.09	0.04	0.04	0.03	0.08	0.06	0.10	0.08
FeO	0.78	0.24	0.32	0.37	0.92	0.45	0.39	0.26	0.85	0.65	1.08	0.86
MgO	0.00	0.00	0.00	0.01	0.06	0.11	0.09	0.00	0.25	0.00	0.07	0.29
MnO	0.23	0.24	0.21	0.18	0.23	0.26	0.25	0.35	0.45	0.42	0.43	0.52
CaO	3.81	4.06	4.03	4.12	3.78	4.05	4.08	4.06	3.64	3.86	3.61	3.71
PbO	0.21	0.20	0.20	0.14	0.13	0.15	0.17	0.30	0.16	0.12	0.13	0.17
Na ₂ O	0.92	0.78	0.81	0.77	0.93	0.81	0.78	0.78	1.06	0.88	1.01	1.10
Li ₂ O	2.45	2.51	2.56	2.56	2.47	2.58	2.45	2.56	2.56	2.57	2.32	2.39
H ₂ O	3.12	3.10	3.16	3.18	3.17	3.20	3.13	3.13	3.20	3.35	3.18	3.13
F	1.43	1.46	1.34	1.37	1.34	1.28	1.35	1.43	1.34	0.86	1.26	1.38
O=F	-0.60	-0.61	-0.56	-0.58	-0.56	-0.54	-0.57	-0.60	-0.56	-0.36	-0.53	-0.58
Σ	100.13	99.72	99.82	100.63	100.31	100.16	99.31	100.33	101.06	98.96	99.80	100.05
Si ⁴⁺ apfu	5.913	5.906	5.923	5.916	5.929	5.939	5.899	5.922	5.973	5.956	5.904	5.919
B ³⁺	3.000	3.000	3.000	3.000	3.000	3.000	3.000	3.000	3.000	3.000	3.000	3.000
Al ³⁺	6.000	6.000	6.000	6.000	6.000	6.000	6.000	6.000	6.000	6.000	6.000	6.000
Ti ⁴⁺	0.005	0.002	0.002	0.002	0.007	0.004	0.004	0.001	0.007	0.010	0.017	0.012
Al ³⁺	1.297	1.335	1.297	1.307	1.251	1.238	1.316	1.293	1.141	1.193	1.271	1.202
Fe ³⁺	0.009	0.003	0.004	0.004	0.011	0.005	0.005	0.003	0.010	0.008	0.012	0.010
Fe ²⁺	0.102	0.031	0.042	0.049	0.121	0.059	0.052	0.035	0.111	0.086	0.143	0.114
Mg ²⁺	0.000	0.000	0.000	0.002	0.014	0.026	0.021	0.000	0.058	0.000	0.017	0.068
Mn ²⁺	0.031	0.032	0.028	0.024	0.031	0.035	0.034	0.047	0.060	0.057	0.058	0.070
Li ⁺	1.556	1.597	1.627	1.612	1.565	1.633	1.568	1.621	1.613	1.646	1.482	1.524
ΣY	3.000	3.000	3.000	3.000	3.000	3.000	3.000	3.000	3.000	3.000	3.000	3.000
Ca ²⁺	0.645	0.688	0.682	0.691	0.638	0.683	0.695	0.684	0.610	0.660	0.614	0.630
Na ⁺	0.282	0.239	0.248	0.234	0.284	0.247	0.240	0.238	0.322	0.272	0.311	0.338
Pb ²⁺	0.009	0.009	0.009	0.006	0.006	0.006	0.007	0.013	0.007	0.005	0.006	0.007
□	0.064	0.064	0.061	0.069	0.072	0.064	0.058	0.065	0.061	0.063	0.069	0.025
ΣX	1.000	1.000	1.000	1.000	1.000	1.000	1.000	1.000	1.000	1.000	1.000	1.000
OH ⁻	3.286	3.270	3.331	3.321	3.332	3.362	3.322	3.288	3.337	3.566	3.367	3.309
F ⁻	0.714	0.730	0.669	0.679	0.668	0.638	0.678	0.712	0.663	0.434	0.633	0.691
$\Sigma(V+W)$	4.000	4.000	4.000	4.000	4.000	4.000	4.000	4.000	4.000	4.000	4.000	4.000

<T-O> versus site occupancy

Ertl *et al.* (2006) refined the occupancies of T-site B in four crystals of elbaite–liddicoatite from Madagascar and presented a relation between the refined ^[4]B content and the corresponding <T–O> values (Fig. 8a). The correlation coefficient given for the relation shown in Figure 8a is 0.984, and the standard error of estimate is 0.001 Å. In considering the agreement between observed data and a model, the deviations of the data from their ideal values of that model should follow a normal distribution. We may examine the deviations between the measurements and their ideal values using half-normal probability-plot analysis (Abrahams 1972, 1974, Abrahams & Keve 1971). If the weighted deviations from the ideal values are drawn from a normal distribution, the ranked weighted observed differences, $\Delta/\sigma\Delta$, should be linear, with the expected normal distri-

bution (defined for small samples by Hamilton & Abrahams 1972), and have a slope of unity and an intercept of zero. Figure 8b shows the resulting relation for the data of Figure 8a; the data are linear but the slope of the relation is 0.12, a factor of ~8 less than the correct value of 1.0. The origin of the error in this type of plot may come from (1) erroneous assignment of standard deviations; (2) some systematic bias in the data. The origin of this bias is not clear. However, what is clear is that this relation between <T–O> and ^[4]B content cannot be considered as firmly established.

Two other relations between <T–O> and site populations have been presented: (1) <T–O> versus ^[4]Al for a series of uvite samples (MacDonald & Hawthorne 1995), and (2) <T–O> versus ^[4]B for a series of tourmaline samples (Hughes *et al.* 2004). Hughes *et al.* (2004) expressed <T–O> solely as a function of ^[4]B where the assigned T-site populations also contain ^[4]Al

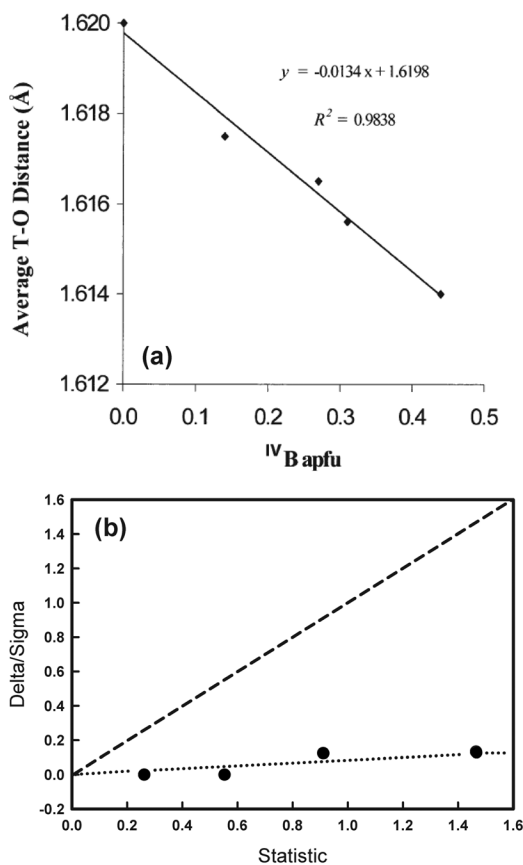


FIG. 8. (a) The relation between $\langle T\text{-O} \rangle$ and ^{14}B content from Ertl *et al.* (2006); (b) half-normal probability plot for the data of Figure 8a; the broken line shows the correct relation, and the dotted line shows a least-squares fit to the data.

and ^{14}Be , and so the status of this relation is not clear. MacDonald & Hawthorne (1995) did not consider the possible presence of ^{14}B in their uvite samples, but Lussier *et al.* (2009) did not detect any ^{14}B in these samples by ^{11}B MAS NMR.

Here, we examine the variation in $\langle T\text{-O} \rangle$ as a function of constituent cation radius (from Shannon 1976) as the effect of each cation is incorporated into the aggregate radius at the T site for each structure. Figure 9 shows the resultant relation for structures from MacDonald & Hawthorne (1995), Schreyer *et al.* (2002), Hughes *et al.* (2000, 2001, 2004), Ertl & Hughes (2002), Ertl *et al.* (1997, 2003a, 2003b, 2004, 2005, 2006, 2007), Marschall *et al.* (2004) and Cempírek *et al.* (2006). What is immediately apparent is that the close fits to linear models presented by MacDonald & Hawthorne (1995), Hughes *et al.* (2004) and Ertl *et*

al. (2006) are not all mutually compatible. Moreover, it is also apparent that the site populations given for several structures are not compatible with the observed mean bond-lengths: For example, the olenite of Ertl *et al.* (1997) (with $^{14}\text{B} = 1.225 \text{ apfu}$) has a much larger ^{14}B content than the olenite of Ertl *et al.* (2007) (with $^{14}\text{B} = 0.660 \text{ apfu}$) and yet has a considerably longer mean bond-length: 1.610 versus 1.604 \AA . Ertl *et al.* (2007) updated the T -site population of the olenite reported by Ertl *et al.* (1997) from $(\text{Si}_{4.775}\text{B}_{1.225})$ to $(\text{Si}_{4.89}\text{B}_{0.83}\text{Al}_{0.27}\text{Be}_{0.01})$, but this proposal is difficult to evaluate, as no new chemical data or structural results are given to justify this reassignment. The scatter of the data in Figure 9 does not warrant doing a least-squares fit. The dashed line was drawn through the data by eye, and the dotted line was drawn through the data of MacDonald & Hawthorne (1995) (no ^{14}B , $T = \text{Si}, \text{Al}$ only) with a slope of ~ 1 . These two lines diverge at low aggregate radii (large ^{14}B values), emphasizing that we need some reliable data for high- ^{14}B tourmalines in order to tie down the lower end of the trends suggested by Figure 9.

The Z site

Hawthorne *et al.* (1993) showed that Al and Mg can be partly disordered over the Y and Z sites. MacDonald & Hawthorne (1995) showed that Mg may occur at the Z site in uvite (ideal formula $\text{Ca}^{\text{Y}}\text{Mg}_3^{\text{Z}}(\text{Al}_5\text{Mg})\text{Si}_6\text{O}_{18}(\text{BO}_3)_3(\text{OH})_3\text{F}$; Hawthorne & Henry 1999). Trivalent Cr is partly disordered over the Y and Z sites (Bosi *et al.* 2004). Taylor *et al.* (1995) showed that incorporation of O^{2-} at the $O(1)$ site can drive disorder of divalent and trivalent cations over the Y and Z sites. Thus it has been established that Al, Fe^{3+} , Cr^{3+} and Mg can occur at the Z site. The situation for Fe^{2+} is more controversial. Hawthorne *et al.* (1993) originally considered the disorder of Mg and Al over the Y and Z sites. The decision to restrict disorder to Mg and Al only was not based on crystal-chemical reasons; they stated that it was done this way because there was no information

TABLE 7. MÖSSBAUER PARAMETERS FOR LIDDICOATITE

	δ (mm/s)	Δ (mm/s)	Γ (mm/s)	Rel. area (%)
$(x^2 = 0.62)$ Prism				
Fe^{2+}	1.080(12)	2.48(5)	0.30(2)	72(34)
Fe^{2+}	1.12(4)	2.23(17)	0.30(8)	23(35)
Fe^{3+}	0.26(11)	0.31(18)	0.28*	5(2)
$(x^2 = 0.54)$ Pyramid				
Fe^{2+}	1.081(8)	2.44(2)	0.29(2)	74(14)
Fe^{2+}	1.14(13)	1.81(45)	0.43(19)	17(18)
Fe^{3+}	0.31(12)	0.27(15)	0.28(12)	9(4)

* fixed parameter.

available on site scattering apart from the fact that previous refinements had been done with $Z = \text{Al}_6 \text{ apfu}$. For tourmalines of the schorl–dravite series, Bloodaxe *et al.* (1999) stated that their refined site-scattering values for the Z site lie in the range 12–13 e (although they did not give the specific values, and did not state what type of scattering factors they used to refine their structures). Accordingly, they assigned only Mg and Al to the Z site for these structures. Conversely, for tourmalines of the schorl–dravite series, Bosi & Lucchesi (2004) reported refined Z-site scattering values in the range 12.87(5)–13.48(7) e and assigned small amounts of Fe^{2+} to the Z site in some (but not all) structures of this series. Finally, Bosi (2008) and Andreozzi *et al.* (2008) put forward a persuasive case for partial disorder of Fe^{2+} over the Y and Z sites in some tourmalines of the schorl–dravite series. What is certain from the above discussion is that other cations in addition to Al can occur at the Z site in the tourmaline structure.

For the crystals of this study, if allowed to vary during refinement, the Z site refined to complete Al occupancy, and it was fixed as such in the final stages of refinement. Equivalent isotropic-displacement parameters are in accord with equal scattering at the Z site in all of the structures refined here [$U_{\text{eq}} = 0.0061(5)$], and the $\langle Z-\text{O} \rangle$ distances are 1.905 ± 0.001 , showing no

significant variation in any of these structures. Moreover, the grand $\langle Z-\text{O} \rangle$ distance of 1.905 \AA and the mean c parameter (~ 7.11 , Table 1) are in close accord with the corresponding curve of Bosi (2008). We thus conclude that the Z site is completely occupied by Al in these structures.

The Y site

Comparison of compositional and structural data confirms that the Y sites are occupied by Li, Al, Fe^{2+} , and Mn^{2+} , with minor-to-trace amounts of Ti^{4+} and Mg. In all samples analyzed, the mean absolute deviation between the refined site-scattering values and the analogous value derived from the unit formulae is 0.5 e per site, indicating very close agreement between the formula-normalization procedure and the proposed site-assignments. The variation in $\langle Y-\text{O} \rangle$ distances with the aggregate radius of the constituent Y-site cations is linear, with no significant deviations (Fig. 10).

The X site

The formulae derived from the chemical compositions (Table 4) have Na, Ca and Pb assigned to the X

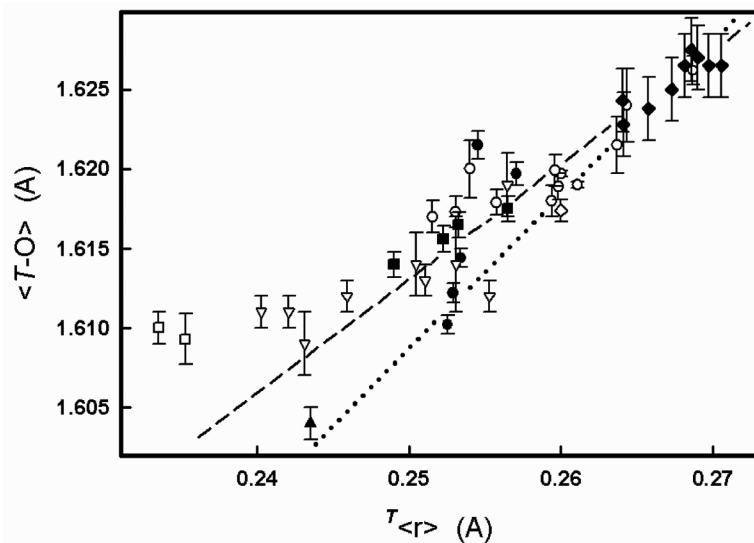


FIG. 9. Variation in $\langle T-\text{O} \rangle$ as a function of constituent-cation radius for selected data from the literature (see text). White circles: Hughes *et al.* (2000, 2001), Schreyer *et al.* (2002), Ertl & Hughes (2002), Ertl *et al.* (2003a, 2003b), Marschall *et al.* (2004), Ertl *et al.* (2005), Cempírek *et al.* (2006); black circles: Hughes *et al.* (2004); black diamonds: MacDonald & Hawthorne (1995); black triangle: Ertl *et al.* (2007); inverted white triangles: Lussier *et al.* (2008); black squares: Ertl *et al.* (2006); white squares: Ertl *et al.* (1997), Hughes *et al.* (2000); white diamond: grand mean value for the 26 structures of the present study. Dashed line: drawn as a guide to the eye through all the data; dotted line: drawn as a guide to the eye through the data of MacDonald & Hawthorne (1995).

site. The X site is almost completely filled, with vacancies that are consistently less than 0.10 $apfu$.

W and V sites

For any tourmaline, the occupancy of the W position [$\equiv O(1)$ site] in the general formula is $[(OH)_xF_{O_{1-x-y}}]$, where $0 \leq x, y \leq 1$ (and $x + y \leq 1$), and the occupancy of the V position [$\equiv O(3)$ site] is $[(OH)_xO_{3-x}]$ where $0 \leq x \leq 3$. The occurrence of F at V has not been shown to occur (see Hawthorne & Henry 1999). For the Madagascar liddicoatite crystals analyzed here, the structural formulae (Table 6) are calculated on the initial assumption that $^W(OH) + ^WF = 1 apfu$ and $^V(OH) = 3 apfu$, and hence $(OH) + F = 4 apfu$. By calculating the average sums of bond valences at the $O(1)$ and $O(3)$ sites for each crystal, the validity of these assumptions can be assessed.

Consider first the occupancy of the $O(1)$ site, which is bonded to the three Y -site cations. For a tourmaline where $^WF = 1 apfu$ or $^WO = 1 apfu$, the sum of bond valences incident from the Y -site cations must be ~ 1.0 and $\sim 2.0 vu$, respectively. Where $^W(OH) = 1.00 apfu$, the sum of bond valences on the oxygen ion is $\sim 1.2 vu$, with the remaining $\sim 0.8 vu$ incident from the H ion. If the assumption that $^W(OH) + ^WF = 1 apfu$ is correct, the average sum of bond valences at $O(1)$ is expected to be between 1.00 and 1.20 vu . Table 6 shows that for all the analyzed crystals, the average occupancy of the W site is $[F_{0.671}(OH)_{0.329}]$, with relatively little variance ($\sigma = 0.062 apfu$). The expected bond-valence sum may be derived as a linear combination of these

two components: this gives a value of $\sim 1.06 vu$. Table 8 shows bond-valence sums at the $O(1)$ site for each crystal, calculated using the curves of Brown & Altermatt (1985) and the observed bond-lengths for the disordered $O(1)$ position (Table 4). Here, the calculation is weighted assuming a random distribution of $Y-WF$ bonds in each sample. Cations with smaller radii (such as Al: 0.535 Å) are assigned to the shorter $Y-O(1)$ bond, whereas cations with larger radii (such as Li: 0.76, Fe^{2+} : 0.78 and Mn^{2+} : 0.83 Å) are assigned to the longer $Y-O(1)$ bond. Calculated values vary between 0.96 and 1.05 vu , with an average value of 1.01 vu . This value is in reasonable accord with the predicted value, validating the assumption that $^W(OH) + ^WF = 1 apfu$.

Similarly, for the $O(3)$ site, incident bond-valence sums are also listed in Table 8. These vary between 1.10 and 1.11 vu , with an average of 1.11 vu . Although lower than the ideal value of 1.20 vu expected for full (OH) occupancy, these values clearly indicate no substantial amount of V^O to be present in these crystals, validating the assumption that $^V(OH) = 3 apfu$.

CONCLUSION

Extensive crystal-structure refinement and ^{11}B and ^{27}Al Magic-Angle-Spinning Nuclear Magnetic Resonance spectroscopy have given no evidence of the presence of tetrahedrally coordinated B or Al at the T site throughout the oscillatory zoned crystal of liddicoatite examined here, and hence Si is equal to 6.00 $apfu$ throughout the crystal. The $\langle Z-O \rangle$ distances and equivalent isotropic-displacement parameters show no

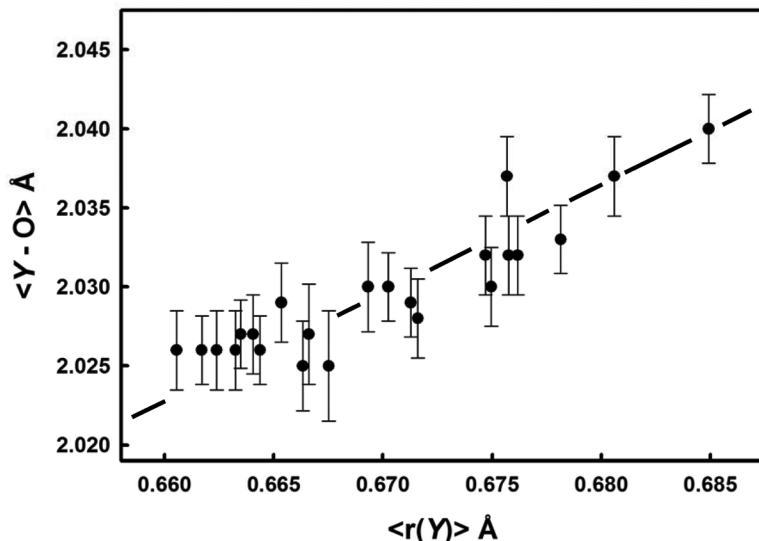


FIG. 10. Variation in $\langle Y-O \rangle$ as a function of the aggregate radius of the cations at the Y site in liddicoatite.

significant variation throughout these structures, and are in accord with complete occupancy of the Z site by Al; thus $Z\text{Al}$ is equal to 6.00 apfu throughout the crystal. We may thus conclude that the oscillatory character of this crystal, which is further characterized by Lussier *et al.* (2011) in an accompanying paper, arises from chemical variations solely at the X and Y sites.

ACKNOWLEDGEMENTS

The authors thank Ferdinando Bosi, Andreas Ertl, Guest Editor Horst Marschall and E.B. for their comments on this paper. We are grateful to Carl Francis, Curator of the Harvard University Mineralogical Museum, for supplying us with this sample. The work was funded by a Canada Research Chair in Crystallography and Mineralogy to FCH, and by a Major Facilities Access Grant, Research Tools and Equipment, and Discovery Grants to FCH and SK from the Natural Sciences and Engineering Research Council of Canada, and by Canada Foundation for Innovation Grants to FCH and SK. Assistance was also provided by funding to AJL in the form of a summer undergraduate NSERC research award, and to AJL and VKM in the form of NSERC Postgraduate Scholarships. Access to the 900 MHz NMR spectrometer was provided by the National Ultrahigh-Field NMR Facility for Solids (Ottawa, Canada), a national research facility funded by the Canada Foundation for Innovation, the Ontario Innovation Trust, Recherche Québec, the National Research Council of Canada, and Bruker BioSpin, and managed by the University of Ottawa (www.nmr900.ca). The Natural Sciences and Engineering Research Council of Canada is acknowledged for a Major Resources Support grant.

TABLE 8. BOND-VALENCE SUMS AT O(1) AND O(3) POSITIONS OF LIDDICOATITE CRYSTALS

Sample	$\Sigma s_{\text{O}(1)}$	$\Sigma s_{\text{O}(3)}$	Sample	$\Sigma s_{\text{O}(1)}$	$\Sigma s_{\text{O}(3)}$
L1	1.00	1.11	L18	1.01	1.10
L2	0.98	1.11	L19	1.02	1.10
L4	1.02	1.11	L20	1.03	1.10
L5	0.97	1.11	L21	1.02	1.10
L6	0.97	1.10	L22	1.02	1.10
L7	0.98	1.11	L23	1.02	1.11
L11	0.98	1.11	L24	1.01	1.10
L12	0.96	1.11	L25	0.97	1.10
L13	1.02	1.11	L26	1.05	1.10
L15	1.01	1.10	L27	1.05	1.11
L16	1.01	1.10	L28	0.98	1.11
L17	1.03	1.10	<vu>	1.01	1.11

The bond-valence sums are expressed in valence units (vu).

REFERENCES

- ABRAHAMS, S.C. (1972): Systematic error differences between two refined sets of position coordinates for $\text{Na}_3\text{PO}_3\text{CO}_2\bullet 6\text{H}_2\text{O}$. *Acta Crystallogr.* **B28**, 2886-2887.
- ABRAHAMS, S.C. (1974): The reliability of crystallographic structural information. *Acta Crystallogr.* **B30**, 261-268.
- ABRAHAMS, S.C. & KEVE, E.T. (1971): Normal probability plot analysis of error in measured and derived quantities and their standard deviations. *Acta Crystallogr.* **A27**, 157-165.
- AGROSI, G., BOSI, F., LUCCHESI, S., MELCHIORRE, G. & SCANDALE, E. (2006): Mn-tourmaline crystals from island of Elba (Italy) growth history and growth marks. *Am. Mineral.* **91**, 944-952.
- AKIZUKI, M., HAMPAR, M.S. & ZUSSMAN, J. (1979): An explanation of anomalous optical properties in topaz. *Mineral. Mag.* **43**, 237-241.
- AKIZUKI, M., KURIBAYASHI, T., NAGASE, T. & KITAKAZE, A. (2001): Triclinic liddicoatite and elbaite in growth sectors of tourmaline from Madagascar. *Am. Mineral.* **86**, 364-369.
- AKIZUKI, M. & SUNAGAWA, I. (1978): Study of the sector structure in adularia by means of optical microscopy, infra-red absorption, and electron microscopy. *Mineral. Mag.* **42**, 453-462.
- AKIZUKI, M. & TERADA, T. (1998): Origin of abnormal optical property of apophyllite. *Neues Jahrb. Mineral., Abh.* **42**, 234-240.
- ANDREOZZI, G.B., BOSI, F. & LONGO, M. (2008): Linking Mössbauer and structural parameters in elbaite - schorl - dravite tourmalines. *Am. Mineral.* **93**, 658-666.
- ASHWAL, L.D. & TUCKER, R.D. (1999): Geology of Madagascar: a brief outline. *Gondwana Res.* **2**, 335-339.
- AURISICCHIO, C., OTTOLINI, L. & PEZZOTTA, F. (1999): Electron- and ion-microprobe analyses, and genetic inferences of tourmalines of the foitite-schorl solid solution. *Eur. J. Mineral.* **11**, 217-225.
- BARTELMEHS, K.L., BLOSS, F.D., DOWNS, R.T. & BIRCH, J.B. (1992): Excalibr II. *Z. Kristallogr.* **199**, 185-196.
- BLOODAXE, E.S., HUGHES, J.M., DYAR, M.D., GREW, E.S. & GUIDOTTI, C.V. (1999): Linking structure and chemistry in the schorl-dravite series. *Am. Mineral.* **84**, 922-928.
- BOSI, F. (2008): Disordering of Fe^{2+} over octahedrally coordinated sites of tourmaline. *Am. Mineral.* **93**, 1647-1653.
- BOSI, F., AGROSI, G., LUCCHESI, S., MELCHIORRE, G. & SCANDALE, E. (2005a): Mn-tourmaline from island of Elba (Italy) crystal chemistry. *Am. Mineral.* **90**, 1661-1668.
- BOSI, F., ANDREOZZI, G.B., FEDERICO, M., GRAZIANI, G. & LUCCHESI, S. (2005b): Crystal chemistry of the elbaite-schorl series. *Am. Mineral.* **90**, 1784-1792.

- BOSI, F. & LUCCHESI, S. (2007): Crystal chemical relationships in the tourmaline group: structural constraints on chemical variability. *Am. Mineral.* **92**, 1054-1063.
- BOSI, F. & LUCCHESI, S. (2004): Crystal chemistry of the schorl-dravite series. *Eur. J. Mineral.* **16**, 335-344.
- BOSI, F., LUCCHESI, S. & REZNITSKII, L. (2004): Crystal chemistry of the dravite-chromdravite series. *Eur. J. Mineral.* **16**, 345-352.
- BRAUN, R. (1891): *Optischen Anomalien der Krystalle*. Bey S. Hirzel, Leipzig, Germany.
- BRAY, P.J., EDWARDS, J.O., O'KEEFE, J.G., ROSS, V.F. & TATSUZAKI, I. (1961): Nuclear magnetic resonance studies of B¹¹ in crystalline borates. *J. Chem. Phys.* **35**, 435-442.
- BROWN, I.D. & ALTERMATT, D. (1985): Bond-valence parameters obtained from a systematic analysis of the Inorganic Crystal Structure Database. *Acta Crystallogr.* **B41**, 244-247.
- BURNS, P.C., MACDONALD, D.J. & HAWTHORNE, F.C. (1994): The crystal chemistry of manganese-bearing elbaite. *Can. Mineral.* **32**, 31-41.
- CÁMARA, F., OTTOLINI, L. & HAWTHORNE, F.C. (2002): Crystal chemistry of three tourmalines by SREF, EMPA, and SIMS. *Am. Mineral.* **87**, 1437-1442.
- CEMPÍREK, J., NOVÁK, M., ERTL, A., HUGHES, J.M., ROSSMAN, G.R. & DYAR, M.D. (2006): Fe-bearing olenite with tetrahedrally coordinated Al from an abyssal pegmatite at Kutná Hora, Czech Republic: structure, crystal chemistry, optical and XANES spectra. *Can. Mineral.* **44**, 23-30.
- ČERNÝ, P. (1982): Anatomy and classification of granitic pegmatites. In *Short Course in Granitic Pegmatites in Science and Industry* (P. Černý, ed.). *Mineral. Assoc. Can., Short Course* **8**, 1-39.
- COLLINS, A.S. & WINDLEY, B.F. (2002): The tectonic evolution of central and northern Madagascar and its place in the final assembly of Gondwana. *J. Geol.* **110**, 325-339.
- COOPER, M.A., HAWTHORNE, F.C. & GREW, E.S. (2009): The crystal chemistry of the kornerupine-prismatic series. I. Crystal structure and site populations. *Can. Mineral.* **47**, 233-262.
- DIRLAM, D.M., LAURS, B.M., PEZZOTTA, R. & SIMMONS, W.B. (2002): Liddicoatite tourmaline from Anjanabonoina, Madagascar. *Gems Gemol.* **38**, 28-53.
- DISSANAYAKE, C.B. & CHANDRAJITH, R. (1999): Sri Lanka – Madagascar Gondwana linkage: evidence for a Pan-African mineral belt. *J. Geol.* **107**, 223-235.
- DUNN, P.J., APPLEMAN, D.E. & NELEN, J. (1977): Liddicoatite, a new calcium end-member of the tourmaline group. *Am. Mineral.* **62**, 1121-1124.
- DUNN, P.J., NELEN, J.A. & APPLEMAN, D.E. (1978): Liddicoatite, a new gem tourmaline species from Madagascar. *J. Gemmol.* **16**, 172-176.
- DYAR, M.D., GUIDOTTI, C.V., CORE, D.P., WEARN, K.M., WISE, M.A., FRANCIS, C.A., JOHNSON, K., BRADY, J.B., ROBERTSON, J.D. & CROSS, L.R. (1999): Stable isotope and crystal chemistry of tourmaline across pegmatite – country rock boundaries at Black Mountain and Mount Mica, southwestern Maine, U.S.A. *Eur. J. Mineral.* **11**, 281-294.
- DYAR, M.D., TAYLOR, M.E., LUTZ, T.M., FRANCIS, C.A., GUIDOTTI, C.V. & WISE, M. (1998): Inclusive chemical characterization of tourmaline: Mössbauer study of Fe valence and site occupancy. *Am. Mineral.* **83**, 848-864.
- ERTL, A. & HUGHES, J.M. (2002): The crystal structure of an aluminum-rich schorl overgrown by boron-rich olenite from Koralpe, Styria, Austria. *Mineral. Petrol.* **75**, 69-78.
- ERTL, A., HUGHES, J.M., BRANDSTÄTTER, F., DYAR, M.D. & PRASAD, P.S.R. (2003b): Disordered Mg-bearing olenite from a granitic pegmatite from Goslar, Austria: a chemical, structural, and infrared spectroscopic study. *Can. Mineral.* **41**, 1363-1370.
- ERTL, A., HUGHES, J.M., PROWATKE, S., LUDWIG, T., BRANDSTÄTTER, F., KÖRNER, W. & DYAR, M.D. (2007): Tetrahedrally coordinated boron in Li-bearing olenite from “mushroom” tourmaline from Momeik, Myanmar. *Can. Mineral.* **45**, 891-899.
- ERTL, A., HUGHES, J.M., PROWATKE, S., LUDWIG, T., PRASAD, P.S.R., BRANDSTÄTTER, F., KÖRNER, W., SCHUSTER, R., PERTLIK, F. & MARSCHALL, H. (2006): Tetrahedrally coordinated boron in tourmalines from the liddicoatite-elbaite series from Madagascar: structure, chemistry, and infrared spectroscopic studies. *Am. Mineral.* **91**, 1847-1856.
- ERTL, A., HUGHES, J.M., PROWATKE, S., ROSSMAN, G.R., LONDON, D. & FRITZ, E.A. (2003a): Mn-rich tourmaline from Austria: structure, chemistry, optical spectra, and relations to synthetic solid solutions. *Am. Mineral.* **88**, 1369-1376.
- ERTL, A., PERTLIK, F. & BERNHARDT, H.-J. (1997): Investigations on olenite with excess boron from the Koralpe, Styria, Austria. *Österreichische Akademie der Wissenschaften, Mathematisch-Naturwissenschaftliche Klasse, Abteilung I, Anzeiger* **134**, 3-10.
- ERTL, A., PERTLIK, F., DYAR, M.D., PROWATKE, S., HUGHES, J.M., LUDWIG, T. & BERNHARDT, H.-J. (2004): Fe-rich olenite with tetrahedrally coordinated Fe³⁺ from Eibenstein, Austria: structural, chemical, and Mössbauer data. *Can. Mineral.* **42**, 1057-1063.
- ERTL, A., ROSSMAN, G.R., HUGHES, J.M., PROWATKE, S. & LUDWIG, T. (2005): Mn-bearing “oxy-rossmanite” with tetrahedrally coordinated Al and B from Austria: structure, chemistry, and infrared and optical spectroscopic study. *Am. Mineral.* **90**, 481-487.
- ERTL, A., TILLMANS, E., NTAFLOS, T., FRANCIS, C., GIESTER, G., KÖRNER, W., HUGHES, J.M., LENGAUER, C. & PREM, M. (2008): Tetrahedrally coordinated boron in Al-rich tourmaline and its relationship to the pressure-temperature conditions of formation. *Eur. J. Mineral.* **20**, 881-888.

- FOORD, E.E. & CUNNINGHAM, C.G. (1978): Thermal transformation of anomalously biaxial dimetric crystals. *Am. Mineral.* **63**, 747-749.
- FOORD, E.E. & MILLS, B.A. (1978): Biaxiality in 'isometric' and 'dimetric' crystals. *Am. Mineral.* **63**, 316-325.
- FRANCIS, C.A., DYAR, M.D., WILLIAMS, M.L. & HUGHES, J.M. (1999): The occurrence and crystal structure of foitite from a tungsten-bearing vein at Copper Mountain, Taos County, New Mexico. *Can. Mineral.* **37**, 1431-1438.
- GORSKAYA, M.G., FRANK-KAMENETSKAYA, O.V., ROZHDESTVENSKAYA, I.V. & FRANK-KAMENETSKII, V.I. (1982): Refinement of the crystal structure of Al-rich elbaite and some aspects of the crystal chemistry of tourmalines. *Sov. Phys. Crystallogr.* **27**, 63-66.
- GRICE, J.D. & ERCIT, T.S. (1993): Ordering of Fe and Mg in the tourmaline crystal structure: the correct formula. *Neues Jahrb. Mineral. Abh.* **165**, 245-266.
- GRICE, J.D., ERCIT, T.S. & HAWTHORNE, F.C. (1993): Povondraite, a redefinition of the tourmaline ferridravite. *Am. Mineral.* **78**, 433-436.
- HAMILTON, W.C. & ABRAHAMS, S.C. (1972): Normal probability plot analysis for small samples. *Acta Crystallogr.* **A28**, 215-218.
- HAWTHORNE, F.C. (1988): Mössbauer Spectroscopy. In *Spectroscopic Methods in Mineralogy and Geology* (F.C. Hawthorne, ed.). *Rev. Mineral.* **18**, 255-340.
- HAWTHORNE, F.C. (1996): Structural mechanisms for light-element variations in tourmaline. *Can. Mineral.* **34**, 123-132.
- HAWTHORNE, F.C. (2002): Bond-valence constraints on the chemical composition of tourmaline. *Can. Mineral.* **40**, 789-797.
- HAWTHORNE, F.C. & HENRY, D.J. (1999): Classification of the minerals of the tourmaline group. *Eur. J. Mineral.* **11**, 201-215.
- HAWTHORNE, F.C., MACDONALD, D.J. & BURNS, P.C. (1993): Reassignment of cation site occupancies in tourmaline: Al-Mg disorder in the crystal structure of dravite. *Am. Mineral.* **78**, 265-270.
- HAWTHORNE, F.C., UNGARETTI, L. & OBERTI, R. (1995): Site populations in minerals: terminology and presentation of results of crystal-structure refinement. *Can. Mineral.* **33**, 907-911.
- HENRY, D.J. & DUTROW, B.L. (1992): Tourmaline in low-grade clastic metasedimentary rock: an example of the petrogenetic potential of tourmaline. *Contrib. Mineral. Petrol.* **112**, 203-218.
- HENRY, D.J. & DUTROW, B.L. (1996): Metamorphic tourmaline and its petrogenetic applications. In *Boron: Mineralogy, Petrology and Geochemistry* (E.S. Grew & L.M. Anovitz, eds.). *Rev. Mineral.* **33**, 503-557.
- HENRY, D.J. & GUIDOTTI, C.V. (1985): Tourmaline as a petrogenetic indicator mineral: an example from the staurolite-grade metapelites of NW Maine. *Am. Mineral.* **70**, 1-15.
- HUGHES, J.M., ERTL, A., DYAR, M.D., GREW, E.S., SHEARER, C.K., YATES, M.G. & GUIDOTTI, C.V. (2000): Tetrahedrally coordinated boron in a tourmaline: boron-rich olenite from Stoffhütte, Koralpe, Austria. *Can. Mineral.* **38**, 861-868.
- HUGHES, J.M., ERTL, A., DYAR, M.D., GREW, E.S., WIEDENBECK, M. & BRANDSTÄTTER, F. (2004): Structural and chemical response to varying ^{14}B content in zoned Fe-bearing olenite from Koralpe, Austria. *Am. Mineral.* **89**, 447-454.
- HUGHES, K.-A., HUGHES, J.M. & DYAR, M.D. (2001): Chemical and structural evidence for $^{14}\text{B} \leftrightarrow ^{14}\text{Si}$ substitution in natural tourmalines. *Eur. J. Mineral.* **13**, 743-747.
- KAHR, B. & MCBRIDE, J.M. (1992): Optically anomalous crystals *Angew. Chemie* **31**, 1-26.
- KIRKPATRICK, R.J. (1988): MAS NMR spectroscopy of minerals and glasses. In *Spectroscopic Methods in Mineralogy and Geology* (F.C. Hawthorne, ed.). *Rev. Mineral.* **18**, 341-403.
- KIRKPATRICK, R.J., OESTRIKE, R., WEISS, C.A., JR., SMITH, K.A. & OLDFIELD, E. (1986): High-resolution ^{27}Al and ^{29}Si NMR spectroscopy of glasses and crystals along the join $\text{CaMgSi}_2\text{O}_6 - \text{CaAl}_2\text{SiO}_6$. *Am. Mineral.* **71**, 705-711.
- KIRKPATRICK, R.J., SMITH, K.A., SCHRAMM, S., TURNER, G. & YANG, W.-H. (1985): Solid-state nuclear magnetic resonance spectroscopy of minerals. *Annu. Rev. Earth Planet. Sci.* **13**, 29-47.
- LACROIX, A. (1922): *Minéralogie de Madagascar, I*. Librairie Maritime et Coloniale, Paris, France.
- LUSSIER, A.J., AGUIAR, P.M., MICHAELIS, V.K., KROEKER, S., HERWIG, S., ABDU, Y. & HAWTHORNE, F.C. (2008a): Mushroom elbaite from the Kat Chay mine, Momeik, near Mogok, Myanmar. I. Crystal chemistry by SREF, EMPA, MAS NMR and Mössbauer spectroscopy. *Mineral. Mag.* **72**, 747-761.
- LUSSIER, A.J. & HAWTHORNE, F.C. (2011): Oscillatory zoned liddicoatite from central Madagascar. II. Compositional variation and substitution mechanisms. *Can. Mineral.* **49**, 89-104.
- LUSSIER, A.J., HAWTHORNE, F.C., AGUIAR, P.M., MICHAELIS, V.K. & KROEKER, S. (2009): The occurrence of tetrahedrally coordinated Al and B in tourmaline: a ^{11}B and ^{27}Al MAS NMR study. *Am. Mineral.* **94**, 785-792.
- LUSSIER, A.J., HAWTHORNE, F.C., HERWIG, S., ABDU, Y., AGUIAR, P.M., MICHAELIS, V.K. & KROEKER, S. (2008b): Mushroom elbaite from the Kat Chay mine, Momeik, near Mogok, Myanmar. II. Zoning and crystal growth. *Mineral. Mag.* **72**, 999-1010.
- MACDONALD, D.J. & HAWTHORNE, F.C. (1995): The crystal chemistry of Si-Al substitution in tourmaline. *Can. Mineral.* **33**, 849-858.

- MACDONALD, D.J., HAWTHORNE, F.C. & GRICE, J.D. (1993): Foitite, $\square\text{Fe}^{2+}(\text{Al},\text{Fe}^{3+})\text{Al}_6\text{Si}_6\text{O}_{18}(\text{BO}_3)_3(\text{OH})_4$, a new alkali-deficient tourmaline: description and crystal structure. *Am. Mineral.* **78**, 1299-1303.
- MADELUNG, A. (1883): Beobachtungen mit Breithaupt's Polarisationsmikroskop. *Z. Kristallogr.* **7**, 73-76.
- MALISA, E. & MUHONGO, S. (1990): Tectonic setting of gemstone mineralization in the Proterozoic metamorphic terrane of the Mozambique Belt in Tanzania. *Precamb. Res.* **46**, 167-176.
- MARLER, B. & ERTL, A. (2002): Nuclear magnetic resonance and infrared spectroscopic study of excess-boron olenite from Koralpe, Styria, Austria. *Am. Mineral.* **87**, 364-367.
- MARSCHALL, H.R., ERTL, A., HUGHES, J.M. & McCAMMON, C. (2004): Metamorphic Na- and OH-rich disordered dravite with tetrahedral boron associated with omphacite, from Syros, Greece: chemistry and structure. *Eur. J. Mineral.* **16**, 817-823.
- NEIVA, A.M.R., SILVA, M., MANUELA, V.G., GOMES, M.E. & ELISA, P. (2007): Crystal chemistry of tourmaline from Variscan granites, associated tin-tungsten- and gold deposits, and associated metamorphic and metasomatic rocks from northern Portugal. *Neues Jahrb. Mineral., Abh.* **184**, 45-76.
- NOVÁK, M. & POVONDRA, P. (1995): Elbaite pegmatites in the Moldanubium: a new subtype of the rare-element class. *Mineral. Petrol.* **55**, 159-176.
- NOVÁK, M., SELWAY, J., ČERNÝ, P., HAWTHORNE, F.C. & OTTOLINI, L. (1999): Tourmaline of the elbaite-dravite series from an elbaite-subtype pegmatite at Blízná, southern Bohemia, Czech Republic. *Eur. J. Mineral.* **11**, 557-568.
- PAQUETTE, J.L. & NÉDÉLEC, A. (1998): A new insight into Pan-African tectonics in the East-West Gondwana collision zone by U-Pb zircon dating of granites from central Madagascar. *Earth Planet. Sci. Lett.* **155**, 45-56.
- PEZZOTTA, F. (1996): Preliminary data on the physical-chemical evolution of the gem-bearing Anjanabonoina pegmatite, central Madagascar. *Geol. Assoc. Can. – Mineral. Assoc. Can., Program Abstr.* **21**, A-75.
- PIECZKA, A. (1999): Statistical interpretation of structural parameters of tourmalines; the ordering of ions in the octahedral sites. *Eur. J. Mineral.* **11**, 243-251.
- POUCHOU, J.L. & PICHOIR, F. (1985): PAP $\phi(pZ)$: procedure for improved quantitative microanalysis. In *Microbeam Analysis* (J.T. Armstrong, ed.). San Francisco Press, San Francisco, California.
- POVONDRA, P. & NOVÁK, M. (1986): Tourmalines in metamorphosed carbonate rocks from western Moravia, Czechoslovakia. *Neues Jahrb. Mineral., Monatsh.*, 273-282.
- SAHAMA, T., VON KNORRING, O. & TÖRNROOS, R. (1979): On tourmaline. *Lithos* **12**, 109-114.
- SCHREYER, W., WODARA, U., MARLER, B., VAN AKEN, P.A., SEIFERT, F. & ROBERT, J.-L. (2002): Synthetic tourmaline (olenite) with excess boron replacing silicon in the tetrahedral site. I. Synthesis conditions, chemical and spectroscopic evidence. *Eur. J. Mineral.* **12**, 529-541.
- SELWAY, J.B., ČERNÝ, P., HAWTHORNE, F.C. & NOVÁK, M. (2000b): The Tanco pegmatite at Bernic Lake, Manitoba. XIV. Internal tourmaline. *Can. Mineral.* **38**, 877-891.
- SELWAY, J.B., NOVÁK, M., ČERNÝ, P. & HAWTHORNE, F.C. (1999): Compositional evolution of tourmaline in lepidolite-subtype pegmatites. *Eur. J. Mineral.* **11**, 569-584.
- SELWAY, J.B., NOVÁK, M., ČERNÝ, P. & HAWTHORNE, F.C. (2000a): The Tanco pegmatite at Bernic Lake, Manitoba. XIII. Exocontact tourmaline. *Can. Mineral.* **38**, 869-976.
- SELWAY, J.B., SMEDS, S.-A., ČERNÝ, P. & HAWTHORNE, F.C. (2002): Compositional evolution of tourmaline in the petalite-subtype Nyköpingssgruvan pegmatites, Utö, Stockholm Archipelago, Sweden. *GFF* **124**, 93-102.
- SHANNON, R.D. (1976): Revised effective ionic radii and systematic studies of interatomic distances in halides and chalcogenides. *Acta Crystallogr.* **A32**, 751-767.
- SHTUKENBERG, A., ROZHDESTVENSKAYA, I., FRANK-KAMENETSKAYA, O., BRONZOVA, J., EULER, H., KIRFEL, A., BANNOVA, I. & ZOLOTAREV, A. (2007): Symmetry and crystal structure of biaxial elbaite-liddicoatite tourmaline from the Transbaikalia region, Russia. *Am. Mineral.* **92**, 675-686.
- TAGG, S.L., CHO, H., DYAR, M.D. & GREW, E.S. (1999): Tetrahedral boron in naturally occurring tourmaline. *Am. Mineral.* **84**, 1451-1455.
- TAYLOR, M.C., COOPER, M.A. & HAWTHORNE, F.C. (1995): Local charge-compensation in hydroxy-deficient uvite. *Can. Mineral.* **33**, 1215-1221.
- TEERTSTRA, D.K., ČERNÝ, P. & OTTOLINI, L. (1999): Stranger in paradise; liddicoatite from the High Grade Dike pegmatite, southeastern Manitoba, Canada. *Eur. J. Mineral.* **11**, 227-235.
- TURNER, G.L., SMITH, K.A., KIRKPATRICK, R.J. & OLDFIELD, E. (1986): Boron-11 nuclear magnetic resonance spectroscopic study of borate and borosilicate minerals and a borosilicate glass. *J. Magnetic Resonance* **67**, 544-550.
- ZAGORSKY, V.E., PERETYAZHKO, I.S., SCHIRYEVNA, V.A. & BOGDANOVA, L.A. (1989): Tourmalines from miarolitic pegmatites in Malkhan Range (Transbaikalia). *Mineral. Zh.* **11**, 44-55 (in Russian).

Received February 2, 2010, revised manuscript accepted November 30, 2010.